

IAC-19-A6.2.8.51075

## VARIANCE-COVARIANCE SIGNIFICANT FIGURE REDUCTION AND ITS EFFECT ON COLLISION PROBABILITY CALCULATION

**Salvatore Alfano**

*Sr. Research Astrodynamist, Center for Space Standards and Innovation, Analytical Graphics Inc., 7150 Campus Drive, Suite 260, Colorado Springs, CO 80920, [salfano@agi.com](mailto:salfano@agi.com)*

### Abstract

A covariance matrix must be positive definite to be proper and useful. Essentially, one desires a sufficient number of digits to avoid unintended loss of information while also using few enough digits to be reasonably convenient. Certain data transmission formats require an elemental reduction in the number of significant figures. Sometimes this reduction can cause an otherwise positive definite covariance matrix to appear semi-definite or indefinite. A multitude of high fidelity, self- and other-generated, positive definite, covariance matrices are examined by reducing the number of significant digits while retesting for positive definiteness and suitability for estimating collision probability metrics. Four individual reduction techniques are studied: rounding all elements, rounding up all elements, truncating all elements, and rounding up all diagonal elements while truncating all off-diagonal elements. Results indicate that, for most cases, at least six significant figures are required.

### I. INTRODUCTION

A covariance matrix must be positive-definite to be proper and useful for such things as collision probability calculations, searching for a specific satellite, determining the frequency of orbit updates, track correlation, assessing sensor contributions, etc. For the purposes of this study, a covariance matrix is a symmetric matrix whose element in the  $\langle i, j \rangle$  position is the covariance between the  $i^{\text{th}}$  and  $j^{\text{th}}$  elements of a random vector. It is not the version represented in sigma-correlation form where the off-diagonals are simply the cross-correlation coefficients.

A symmetric matrix is said to be positive definite if all its eigenvalues are strictly positive<sup>1</sup>. Whether it be a 3x3 position covariance matrix, a 6x6 position/velocity covariance matrix, or even a higher-ordered matrix containing additional information regarding time and/or drag and/or other pertinent parameters, an indefinite or semi-definite or negative definite matrix will not yield meaningful results for collision probability or other calculations. This is especially noticeable in visualizing a 3x3 non-positive definite (NPD) positional covariance matrix because it will create a degenerate quadric surface<sup>2</sup> rather than an ellipsoid.

A covariance is a measure of the joint variability of two random variables, providing a measure of the strength of the correlation between the two<sup>3</sup>. If two variables are correlated, then their covariance will be nonzero with the magnitude of the correlation coefficient revealing the strength of the relationship. An  $n \times n$  covariance matrix  $C$  is said to be positive definite if  $y^T C y > 0$  for all non-zero  $y$  in  $\mathbb{R}^n$ . A straightforward test involves determining  $C$ 's eigenvalues; if they are real and positive then the matrix is positive definite<sup>4</sup>.

Typically, an orbit determination system that determines state vector uncertainties will be self-consistent. That is to say, the covariance matrix will be positive definite, containing the same number of significant figures as the states it represents as determined by the computing device. However, certain data transmission formats require an elemental reduction in the number of significant figures, sometimes causing the abbreviated covariance matrix to become semi-definite or indefinite. Sometimes this reduction in significant figures is caused by a reluctance on the part of the message sender to share many significant figures rather than any data transmission format constraint. As well, certain covariance interpolation and/or state transformation techniques can also yield non-positive definite matrices.

It should be noted that positive definiteness is necessary but not sufficient to properly represent uncertainty. A positive-definite covariance matrix can yield improper intermediate eigenvalues and eigenvectors if inappropriate interpolation and/or state transformation techniques are used. Interpolation of individual covariance matrix elements (e.g. using a simple polynomial interpolation) can fail to capture the orbital interdependency between elements and may lead to distortion. Interpolation should be done using rigorous numerical techniques<sup>5,6,7</sup>. It is also advantageous to use an orbit-relative reference frame with sufficiently small step size to minimize covariance elemental rates of change.

The Space Data Center<sup>8</sup> (SDC) occasionally receives Conjunction Data Messages<sup>9</sup> (CDMs) that have NPD covariances, thus preventing a meaningful collision

probability ( $P_c$ ) calculation. There are useful methods available to remediate such occurrences<sup>6</sup>.

This paper examines the effects of four individual reduction techniques and their influence on positive definiteness: rounding all elements, rounding up all elements, truncating all elements, and rounding up all diagonal elements while truncating all off-diagonal elements. Covariance matrices that do not remain positive definite are also examined by ‘repairing’ them using the Eigenvalue Clipping Method detailed in Reference 6. Likewise (and perhaps more importantly), the number of significant digits required to perform  $P_c$  calculations for safety of flight purposes is examined.

## II. SIGNIFICANT FIGURES (DIGITS)

Significant figures indicate the certainty of a measurement or calculation. These are the digits in a value that are known with some degree of confidence. As their number increases, the more certain the calculation becomes. The more precise a measurement, the greater the number of significant figures. There are conventions for expressing numbers so that their significant figures are properly indicated<sup>10</sup>:

- All non-zero digits are significant
- Zeros between non zero digits are significant
- Zeros to the left of the first non-zero digit are not significant
  - Trailing zeros (the right most zeros) are significant when there is a decimal point in the number
  - Trailing zeros are not significant in numbers without decimal points
  - Exact numbers have an infinite number of significant digits but they are generally not reported
  - Defined numbers also have an infinite number of significant digits

When a value contains more significant figures than needed, it can be reduced. There are several commonly used methods for this reduction.

- (1) Method 1 involves simple rounding. The last digit you wish to keep is left the same if the next digit is less than 5, and is increased by 1 if the next digit is 5 or more (henceforth referred to as ‘rounding’),
- (2) Method 2 involves rounding up all elements. The last digit you wish to keep is left the same if the following digits are all 0, and is increased by 1 otherwise (subsequently referred to as ‘rounding up’),
- (3) Method 3 involves truncating all elements. The last digit you wish to keep is simply left unchanged (hereafter referred to as ‘truncation’),
- (4) Method 4 is a hybrid approach that rounds up the variances (diagonal elements) and truncates the

covariances (off-diagonal elements). This will be referred to as the ‘hybrid approach.’

For the purposes of this work, the above methods will be used when a value is positive. For a negative value, these methods will be applied to the absolute value and the result will be given a negative sign. This means that rounding up causes a value to become further away from zero and rounding down (truncating) causes a value to become closer to zero.

The effect of the four methods when applied to each and every element  $c_{i,j}$  in a 3x3 position covariance matrix  $C$  is then examined. Once a reduction method is applied to  $C$  for a specified number of significant digits, nearness of the reduced matrix to the full one is determined from the Frobenius norm<sup>11</sup>  $c_F$  where  $\|c_F\|^2 = \sum_{i,j} (c_{i,j}^2)$ . Additionally, effects of the four methods are observed regarding the  $P_c$  calculation for linear relative motion when applied to the elements of a 2x2 covariance matrix in the encounter plane<sup>12</sup> using both CDM and self-generated data.

## III. CDM ANALYSIS

Positive definiteness of covariance matrices is a “necessary but not sufficient” condition. That is, while covariances must be positive definite, the real end goal is to determine how suitable such covariances are for generating collision probability estimates. In order to determine the real-world degradation that reduced digits of precision can cause, CDMs spanning all orbit regimes over a three-year period from April 2014 to May 2017 were analysed. Each of the 975,735 CDMs represented a single conjunction, providing position and velocity vectors for both objects at time of closest approach (TCA); typically, covariance data was also included. This three-year data set contained 1,704,831 covariance matrices, of which 1,701,091 positional 3x3 matrices were positive definite (99.78% of total).

The aspect ratios ( $AR$ ) of the ellipsoids generated by the positive definite covariances were characterized, where  $AR_{max}$  and  $AR_{mid}$  are defined as the ratios of the major-to-minor axes and the mid-to-minor axes, respectively. The analysis revealed that  $AR_{max}$  and  $AR_{mid}$  were slightly skewed toward one. Upon further examination, some of the covariance matrices contained what appeared to be default parameters consisting only of diagonal elements each with a value of  $4.07 \times 10^{15} \text{ m}^2$ . Because the off-diagonal elements were all zero, those covariance matrices will always remain positive definite during significant figure reduction and the aspect ratios will always be equal to one. Eliminating those special cases, 1,690,217 remained (99.36% of positive definite matrices, 99.14% of total). These remaining cases were then binned by rounding the aspect ratios to the nearest digit and determining the percent of occurrence for each bin. Partial results are shown in the 3D and 2D density

plots of Figure 1. Although a few aspect ratios with values as high as 80,000 were observed, only those with  $AR_{max} \leq 60$  and  $AR_{mid} \leq 5$  are displayed for ease of viewing. These 290 bins contain the highest concentration of all occurrences (approximately 50%). Beyond these limits, subsequent bins simply produced a

flat, dark, purple surface with a maximum singular bin occurrence of only 0.0969%, making their visual characterization inconsequential.

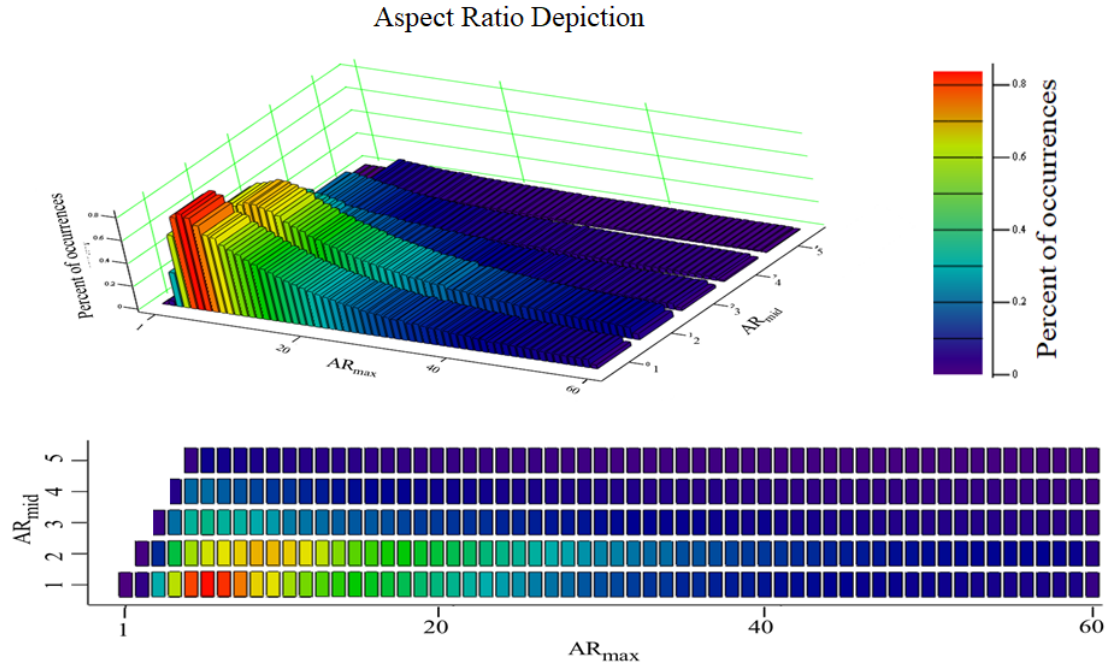


Fig. 1 Binned percent of occurrence for CDM Aspect Ratios ( $AR_{max} \leq 60$  and  $AR_{mid} \leq 5$ )

This was followed by examining how each reduction method effected the positive definiteness of the 3x3  $C$  matrices. If the  $C$  matrices remained such, the nearness of the reduced matrices to the full ones were examined using the Frobenius norm. In Figures 2-5, the graph on the left relates the number of significant figures to the percentage of CDM 3x3 covariance matrices that remained positive definite; as the number of significant figures increases, more and more  $C$  matrices remain

positive definite. The graph on the right shows a composite of the relative differences of the Frobenius norms, represented as mean (in red) and one-sigma standard deviation (depicted as error bounds in blue). As the number of significant figures increases, the Frobenius norm differences decrease. Dashed lines are included to aid the viewer in following the progression; they are not meant for interpolation.

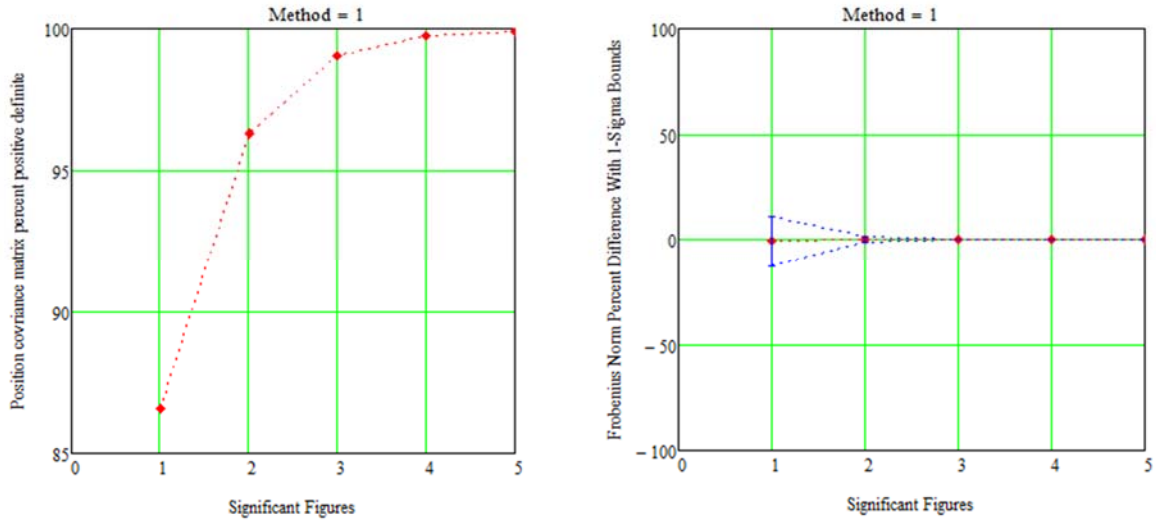


Fig. 2 Method 1 (rounding) significant figure reduction results.

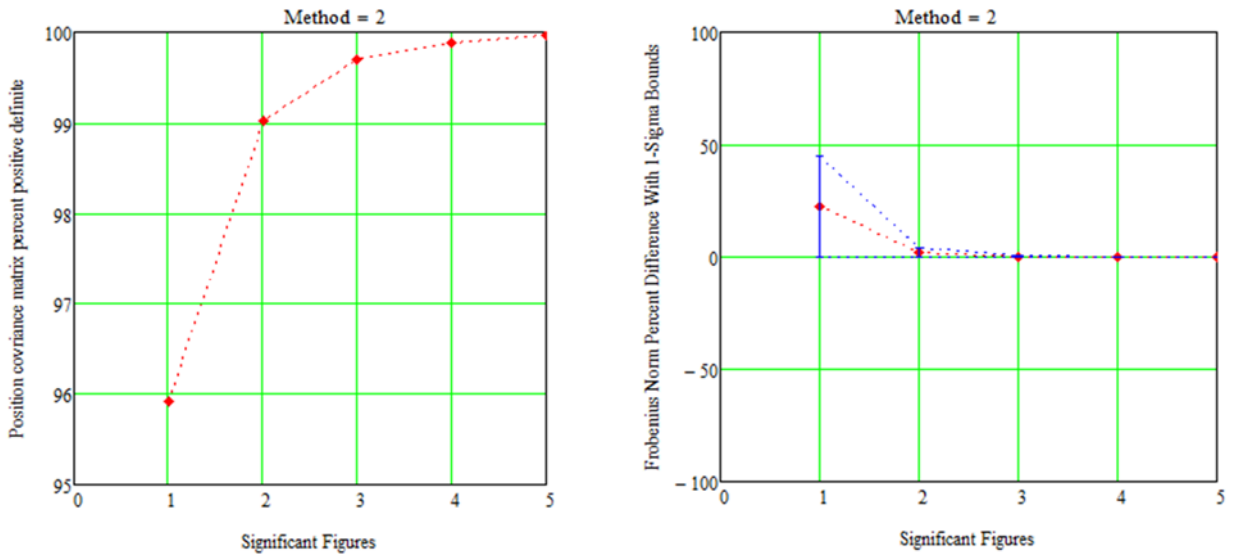


Fig. 3 Method 2 (rounding up) significant figure reduction results.

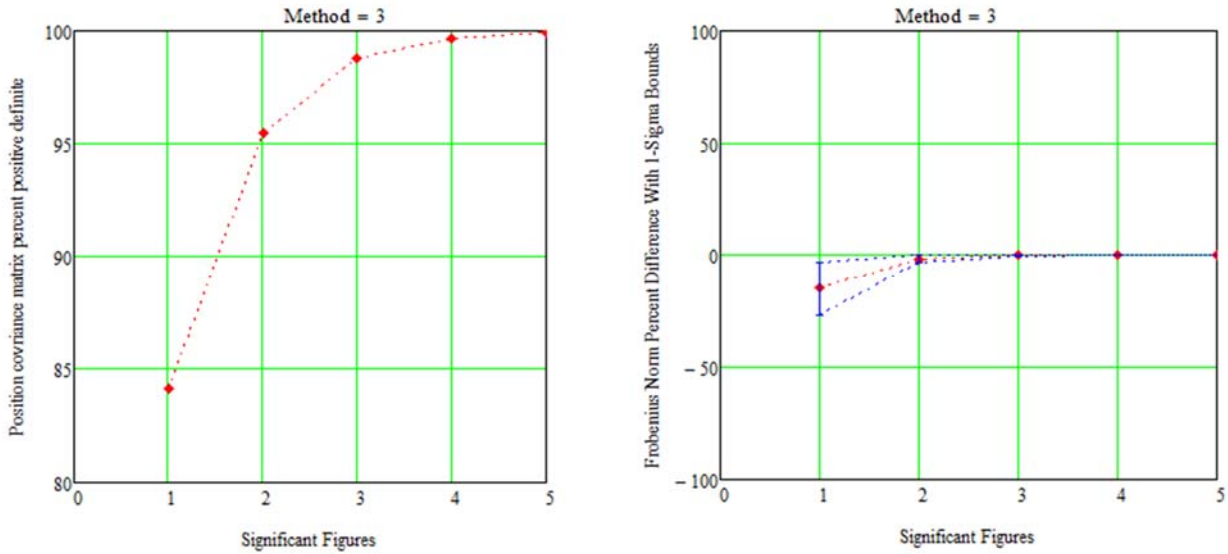


Fig. 4 Method 3 (truncating) significant figure reduction results.

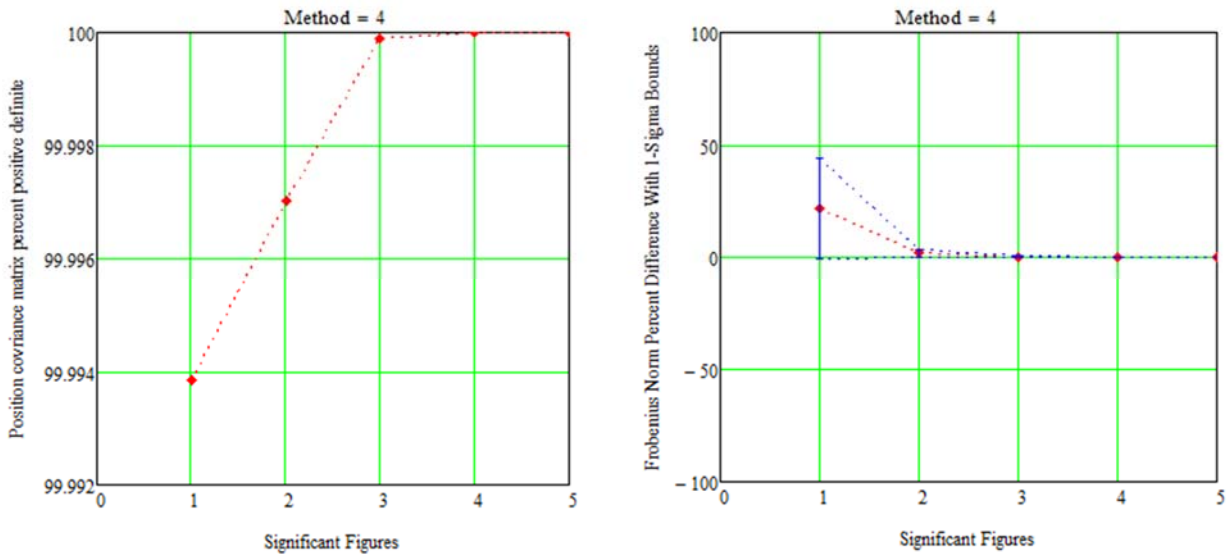


Fig. 5 Method 4 (hybrid approach) significant figure reduction results.

From these figures one can see that in all the methods, three or more significant figures produce good Frobenius Norm agreement, but at least five significant figures are needed to ensure the CDM covariances remain positive definite. It should be noted that only position covariances at TCA are being examined; no consideration is made regarding the effects of propagation, interpolation, or velocity uncertainties; positive definiteness of full 6x6 covariances is also of concern.

The previous figures dealt with covariance matrices that remained positive definite after reduction. Covariance matrices that did not remain positive definite were then examined separately by ‘repairing’ them using the Eigenvalue Clipping Method detailed in Reference 6. The analysis was repeated on those remediated matrices to produce the following figures.

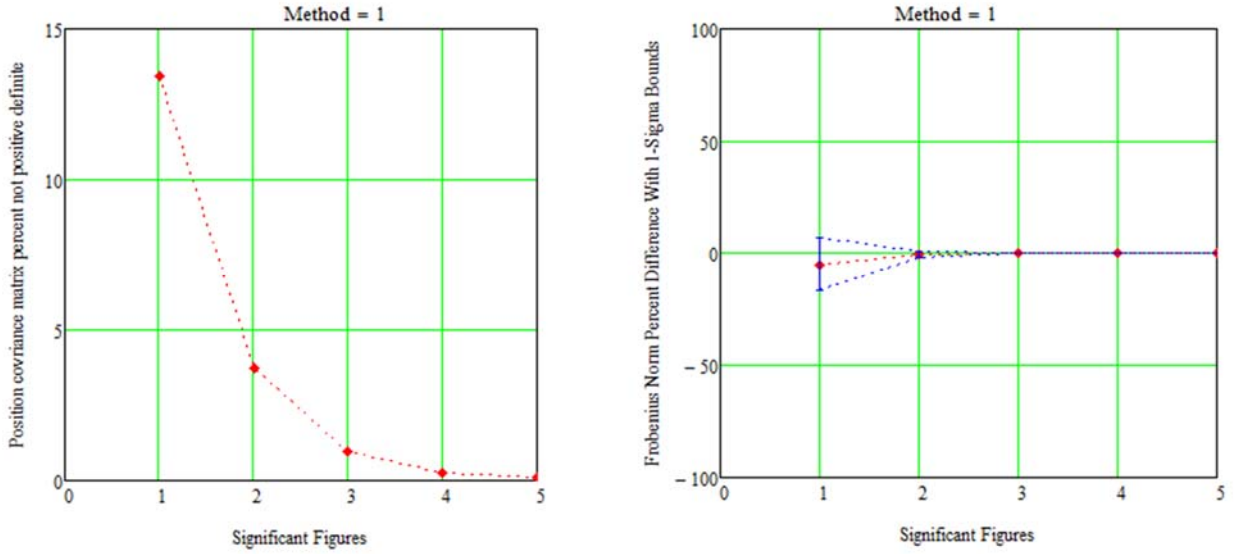


Fig. 6 Method 1 (rounding) significant figure reduction results after repair.

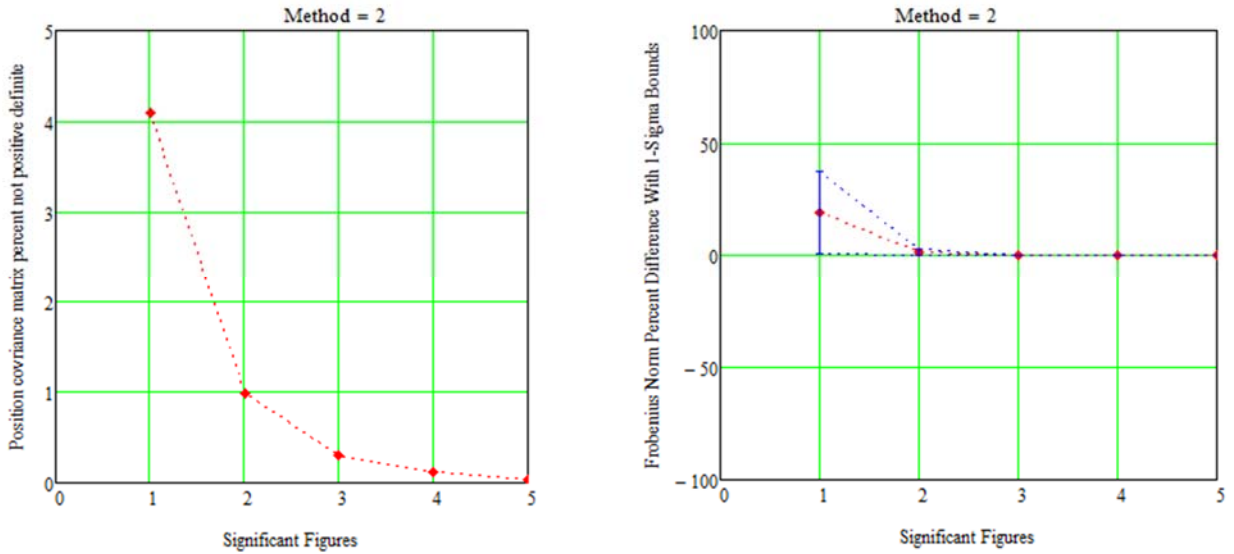


Fig. 7 Method 2 (rounding up) significant figure reduction results after repair.

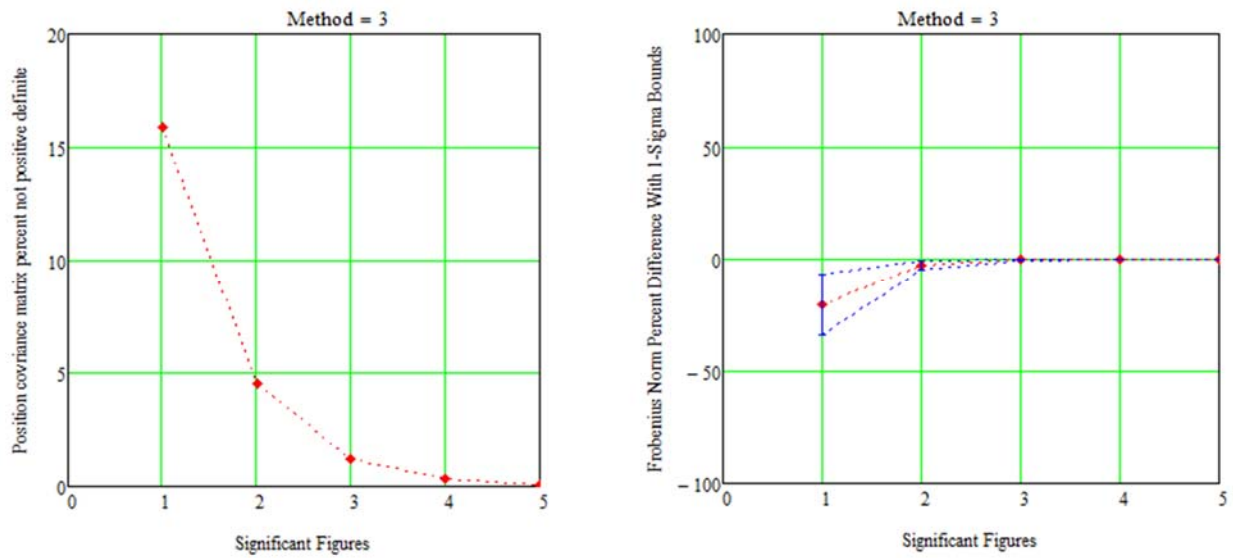


Fig. 8 Method 3 (truncating) significant figure reduction results after repair.

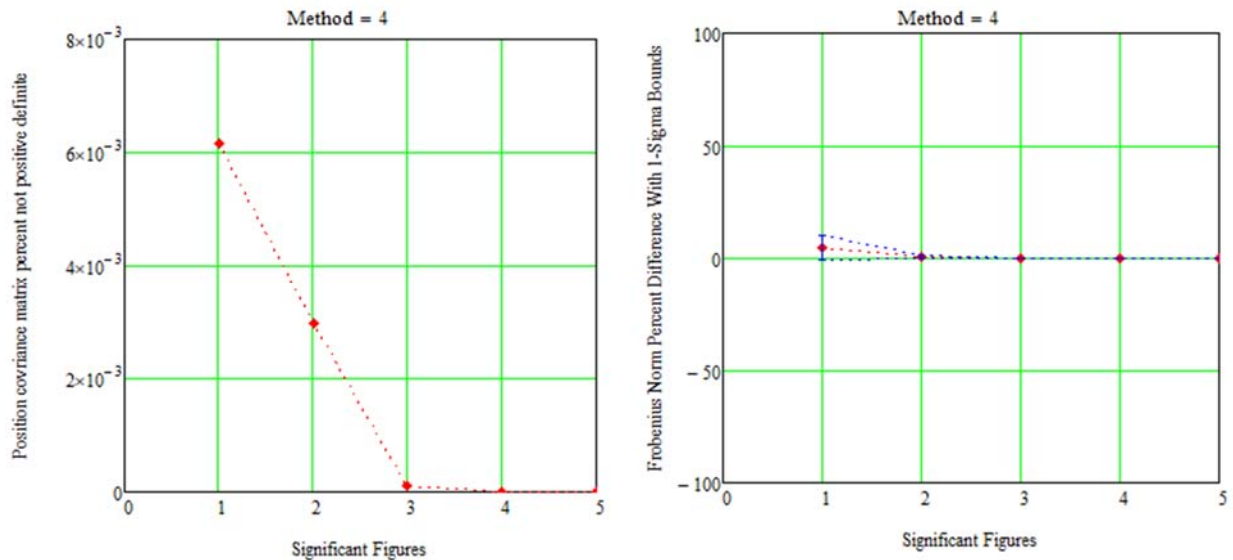


Fig. 9 Method 4 (hybrid approach) significant figure reduction results after repair.

For the repaired covariance matrices, it is clear that three or more significant figures are needed to produce good Frobenius Norm agreement. This is consistent with the previous results.

#### IV. EFFECTS ON COLLISION PROBABILITY CALCULATION

The CDM data set was then used to determine significant figure reduction effects on collision probability calculations. Reference 12 defined an operational decision making region as collision

probability ranging from  $10^{-1}$  and  $10^{-7}$ . Based on this region, consideration was only given to the effects on probabilities greater than  $10^{-7}$ . A total of 729,498 CDMs (74.8% of total) had sufficient data to perform the calculations. Of those, only 13,187 produced probabilities greater than  $10^{-7}$  (1.4% of total).

To simplify the calculations after reduction, the encounter plane axes were reoriented to align with the covariance ellipse major and minor axes and the miss distance vector rotated accordingly. The reoriented parameters were then directly inserted in to MATHCAD

15 using the two-dimensional collision probability equation

$$P_c = \frac{1}{2\pi\sigma_x\sigma_y} \int_{-OBJ}^{OBJ} \int_{-\sqrt{OBJ^2-x^2}}^{\sqrt{OBJ^2-x^2}} e^{-\frac{1}{2}\left[\left(\frac{x+xm}{\sigma_x}\right)^2 + \left(\frac{y+ym}{\sigma_y}\right)^2\right]} dydx. \quad [1]$$

MATHCAD's computational tolerance was set to the smallest value that would still allow convergence of the double integral in Equation (1) where *OBJ* is the combined object radius, *x* lies along the minor axis, *y* lies along the major axis, *xm* and *ym* are the respective components of the projected miss distance, and  $\sigma_x$  and  $\sigma_y$  are the corresponding standard deviations. For all cases, the MATHCAD 15 tolerance was set to  $10^{-9}$

thereby guaranteeing accuracy to at least nine decimal places (as opposed to nine significant figures). The following figure reflects all 13,187 CDMs; those that remained positive definite as well as those that were remediated. The relative percent error is depicted in red. Also shown in blue is the error's one-sigma standard deviation. To make the plots more readable, all plots have the error data clipped at 100%.

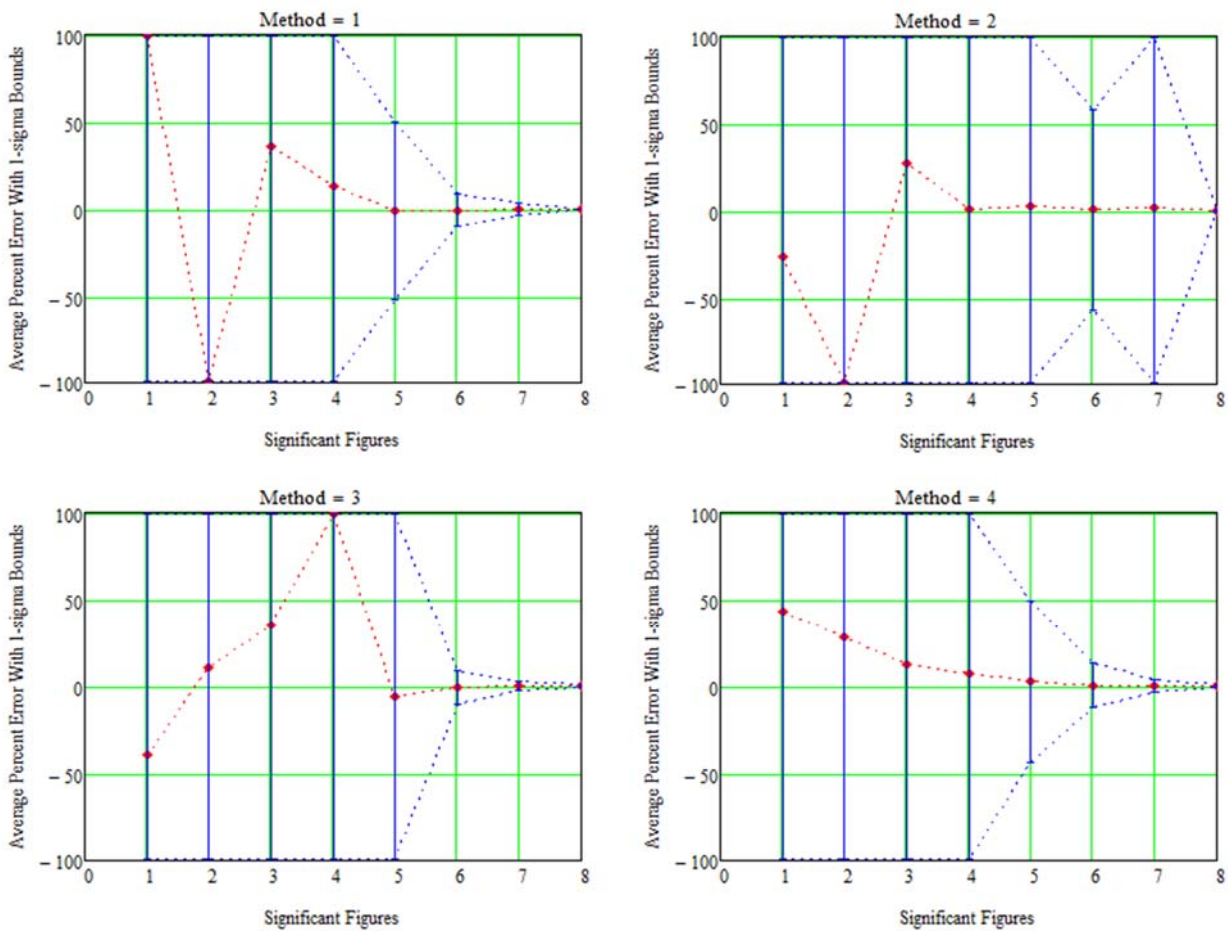


Fig. 10 Representative case for  $P_c > 10^{-7}$  calculation error using the four methods on CDMs.

For  $P_c$  greater than  $10^{-7}$ , it appears that seven or eight significant figures are required depending on allowable error.

The following figure shows the same analysis assuming a typical manoeuvre action threshold of  $P_c$

greater than  $10^{-4}$ . Only 153 CDMs produced probabilities greater than  $10^{-4}$  (0.016% of total). For those cases, it appears that only four or five significant figure are required.

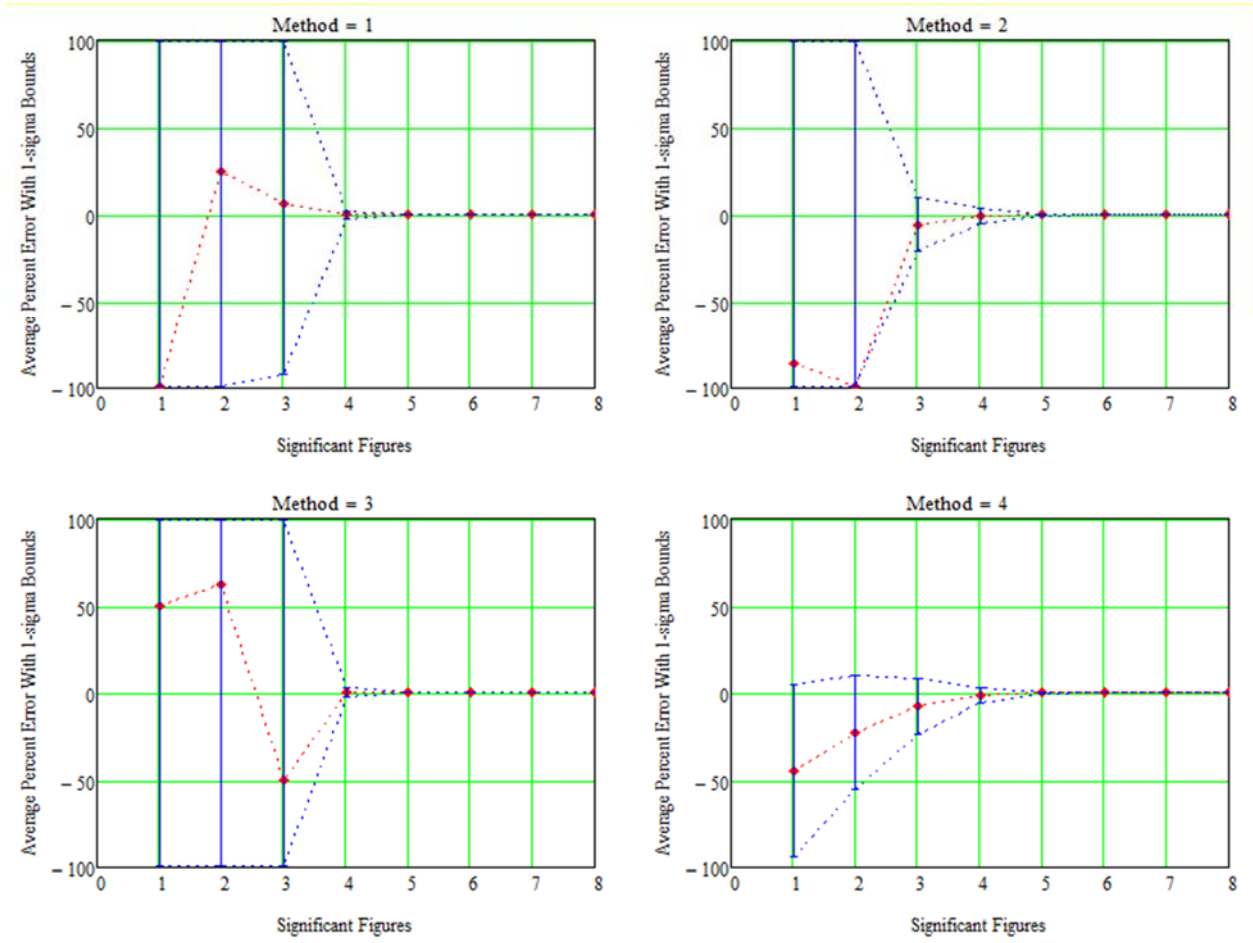


Fig. 11 Representative case for  $P_c > 10^{-4}$  calculation error using the four methods on CDMs.

Because the admissible CDM data sets might be considered sparse for the previous analyses, the study was repeated using the 60,000 self-generated test cases of Reference 12, distributed by aspect ratio to observe its effects. These cases had all parameters normalized to the encounter plane-mapped covariance ellipse's minor-axis standard-deviation of 1. In this normalized space, the object sizes varied from  $10^{-3}$  to  $10^{+3}$ , the miss distance varied from  $10^{-4}$  to  $10^{+3}$  with position ranging from  $0^0$  to  $90^0$  relative to the minor axis, and the covariance ellipse's major-axis standard-deviation varied from 1 to 500 (1

$\leq AR \leq 500$ ). Only those covariance matrices that remained positive definite were examined. The following figure shows a single representative case of relative percent error for  $P_c > 10^{-7}$ ,  $AR=10$ , and each object's normalized radius  $OBJ$  smaller than the normalized miss distance  $d$ . As before, the relative percent error is depicted in red and its one-sigma standard deviation is shown in blue with the error data clipped at 100%.

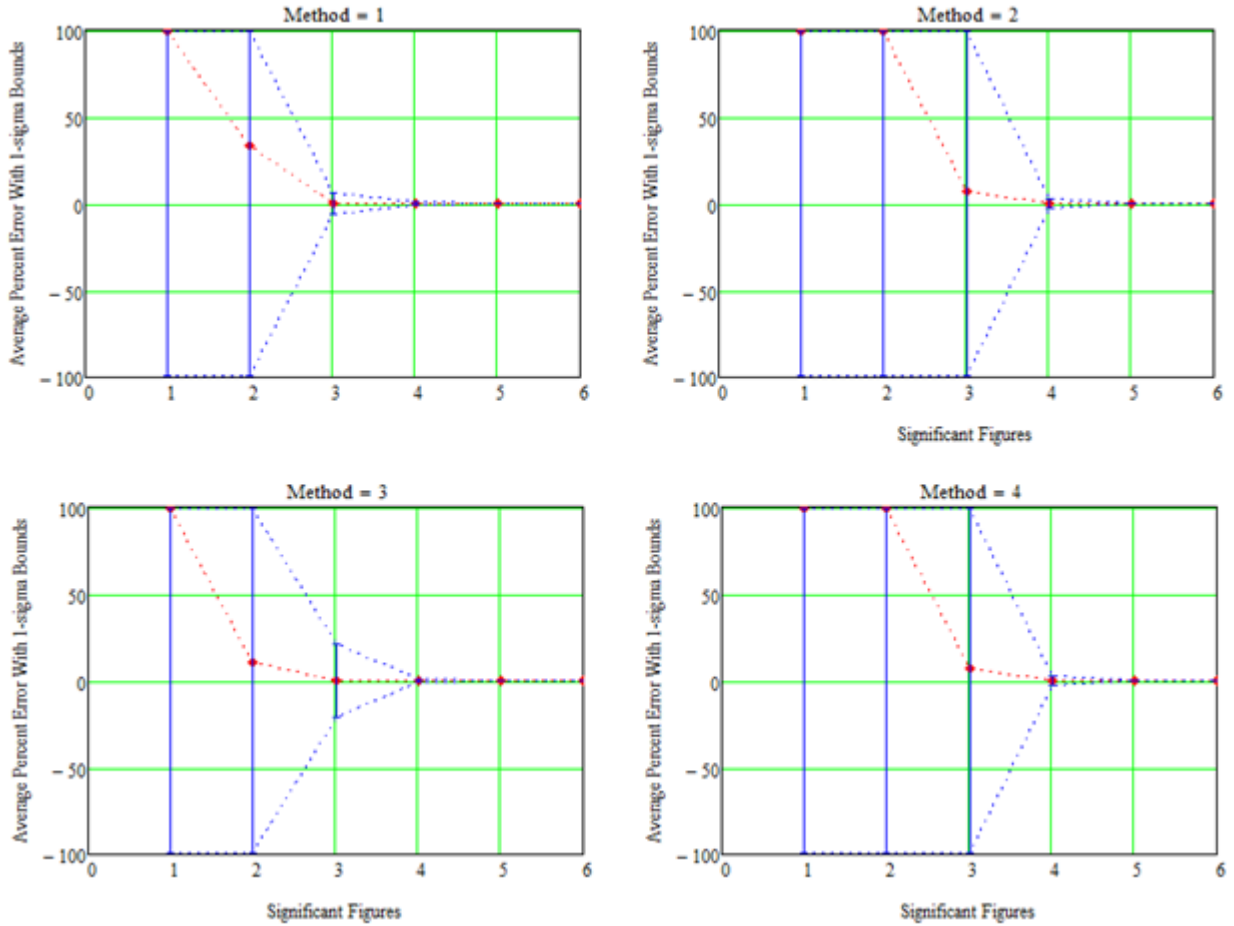


Fig. 12  $P_c$  error for covariances that remained positive definite ( $P_c > 10^{-7}$ ,  $OBJ \leq d$ ,  $AR = 10$ ).

A complete set of figures with  $AR$  of 1, 2, 3, 5, 10, 50, and 500 can be found for all four methods in Appendix A. The appendix figures reveal that at least six significant figures are needed to ensure accurate probability calculations. For objects that have aspect ratios greater than 50, seven significant figures are required.

The following figure shows the relative percent error when including the remediated covariance matrices for  $AR = 10$  with object radii smaller than the miss distance for probabilities greater than  $10^{-7}$ . A complete set of figures can be found in Appendix B. As before, the appendix figures reveal that at least six significant figures are needed to ensure accurate probability calculations.

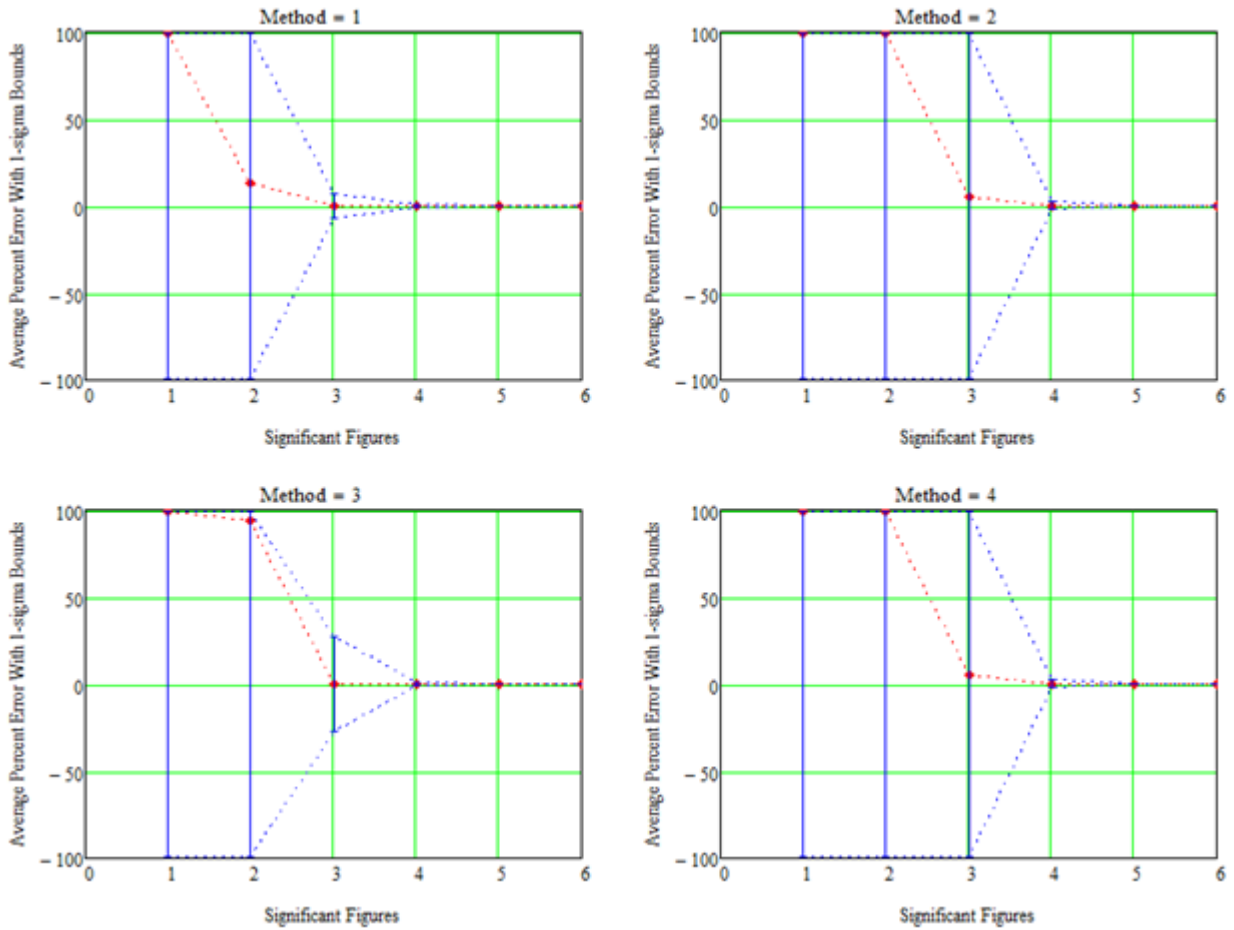


Fig. 13  $P_c$  error for positive definite + remediated covariance matrices ( $P_c > 10^{-7}$ ,  $OBJ \leq d$ ,  $AR = 10$ ).

This analysis was again repeated based on a manoeuvre action threshold of  $10^{-4}$  or greater. The following figure shows the relative percent error for all covariance matrices (remediated and those that remained positive definite) for  $AR = 10$  with object radii smaller

than the miss distance for probabilities greater than  $10^{-4}$ . A complete set of figures can be found in Appendix C. Again, the appendix figures reveal that as many as six significant figures are needed to ensure accurate probability calculations.

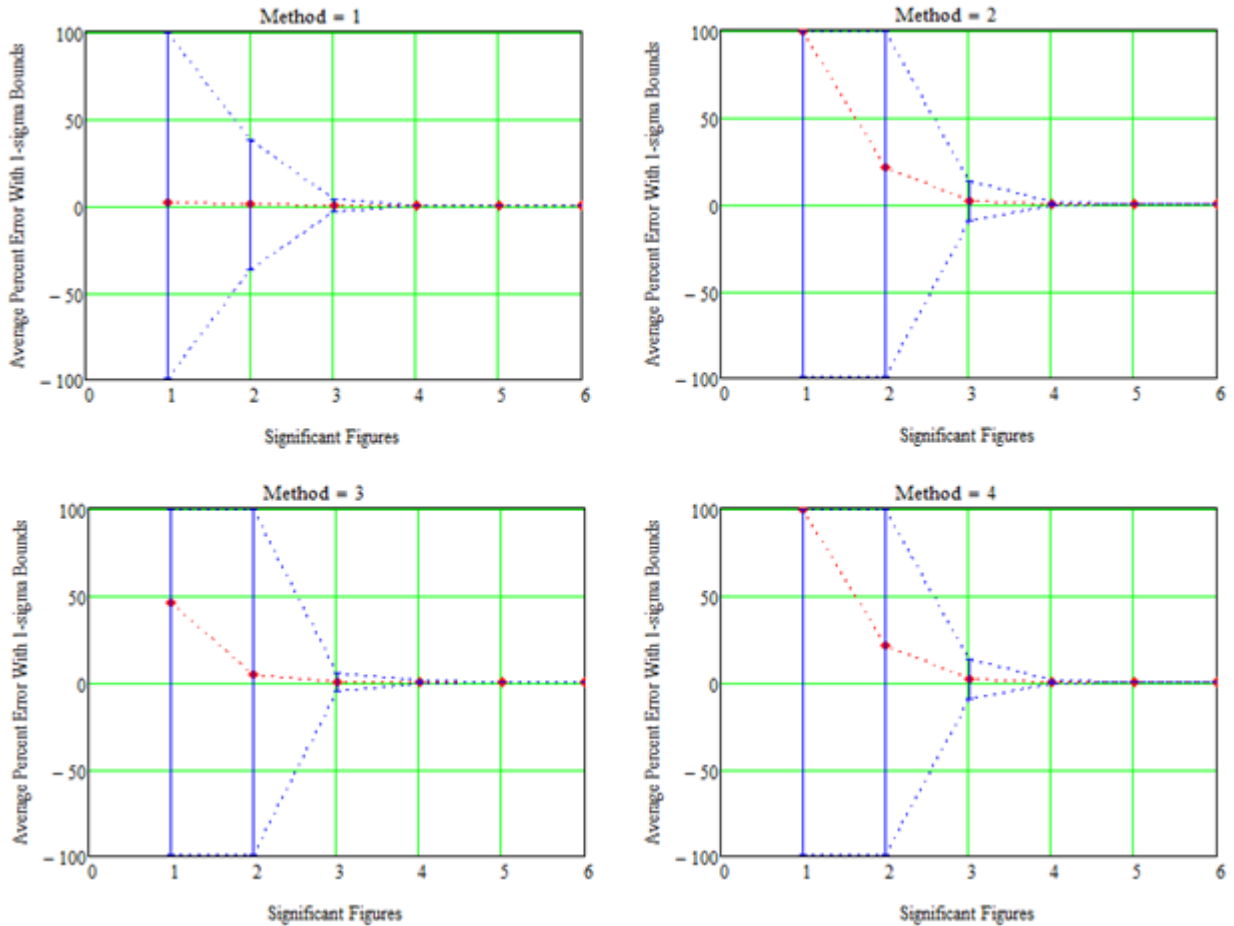


Fig. 14  $P_c$  error for positive definite + remediated covariance matrices ( $P_c > 10^{-4}$ ,  $OBJ \leq d$ ,  $AR = 10$ ).

## V. ACKNOWLEDGEMENTS

I would like to thank my fellow CSSI teammates Dan Oltrogge, T.S. Kelso, and Dave Vallado for contributing to this work. Dan suggested and shaped the research on this topic. T.S. distilled the necessary CDM data in to a more palatable format. Dave suggested various ideas as to what metrics might be useful for operators.

I also wish to express my gratitude to US STRATCOM and 18SPCS for authorizing me to share SP-derived precision assessments with the space operations community to help facilitate understanding.

## VI. CONCLUSION

A multitude of high fidelity, self- and other-generated, positive definite covariance matrices were examined, reducing the number of significant digits while retesting for positive definiteness. Four individual

reduction techniques were studied: rounding all elements, rounding up all elements, truncating all elements, and rounding up all diagonal elements while truncating all off-diagonal elements. A determination was made that at least six significant figures are needed to maintain positive definiteness while, after remediation, only three are needed for good Frobenius Norm agreement.

Also examined were the number of significant digits required for collision probability calculation. The results show that, for higher-probability events, four or more significant figures are needed to ensure actionable, accurate probability calculations depending the aspect ratio as observed in the encounter plane. For lower probability events, at least seven significant figures are needed.

## References

- <sup>1</sup> Hildebrand, F.B., *Introduction to Numerical Analysis*, 2<sup>nd</sup> ed., Dover Publications, Inc. New York, NY, USA ©1987, ISBN:0-486-65363-3, p. 644.
- <sup>2</sup> Alfano, S., and Greer, M.L., "Determining if Two Solid Ellipsoids Intersect," with *AIAA Journal of Guidance, Control, and Dynamics*, Vol. 26, No. 1, January-February 2003, pp. 106-110.
- <sup>3</sup> Rice, J., *Mathematical Statistics and Data Analysis (2007)*, Belmont, CA, Brooks/Cole Cengage Learning. ISBN 978-0534-39942-9, p. 138.
- <sup>4</sup> Lucas, C., Computing Nearest Covariance and Correlation Matrices, University of Manchester, School of Mathematics Thesis, 2001.
- <sup>5</sup> Alfano, S., "Orbital Covariance Interpolation," Paper No. AAS 04-223, AAS/AIAA Spaceflight Mechanics Meeting, Feb 8-12, 2004.
- <sup>6</sup> Hall, D.T., Hejduk, M.D., and Johnson, L.C., "Remediating Non-Positive Definite State Covariances For Collision Probability Estimation," *Advances in the Astronautical Sciences Astrodynamics 2017*, Volume 162, AAS 17-567.
- <sup>7</sup> Woodburn, J., and Tanygin, S., "Position Covariance Visualization," Paper No. AIAA 2002-4985, AIAA/AAS Astrodynamics Specialist Conference and Exhibit, 5-8 August 2002, Monterey, California.
- <sup>8</sup> <https://www.space-data.org/sda/space-data-center-3/> as of Feb 28, 2019.
- <sup>9</sup> Conjunction Data Message, Recommended Standard, CCSDS 508.0-B-1, Blue Book, June 2013, <https://public.ccsds.org/Pubs/508x0b1e2s.pdf> as of Jan 16, 2019.
- <sup>10</sup> Significant Figures (Digits), <https://www.nde-ed.org/GeneralResources/SigFigs/SigFigs.htm> as of Jan 16, 1017
- <sup>11</sup> Ford, W., *Numerical Linear Algebra with Applications Using MATLAB*, Elsevier, Waltham, MA, USA, 2015, ISBN 978-0-12-394435-1.
- <sup>12</sup> Alfano, S., "Review of Conjunction Probability Methods for Short-term Encounters," Paper No. AAS 07-148, AAS/AIAA Space Flight Mechanics Meeting, Sedona, Arizona, Jan 28 – Feb 1, 2007.

## Appendix A

The following figures show the effects of significant figure reduction on collision probability calculations using all four methods for collision probabilities of  $10^{-7}$  or greater:

- 1) rounding all elements,
- 2) rounding up all elements,
- 3) truncating all elements, and
- 4) the hybrid approach (rounds up diagonal elements and truncates off-diagonal elements)).

After the methods were applied, only those matrices that remained positive definite were examined. Relative percent errors are depicted in red. The error's one-sigma standard deviation is shown in blue. To make the plots more readable, all plots have the error data clipped at 100%.

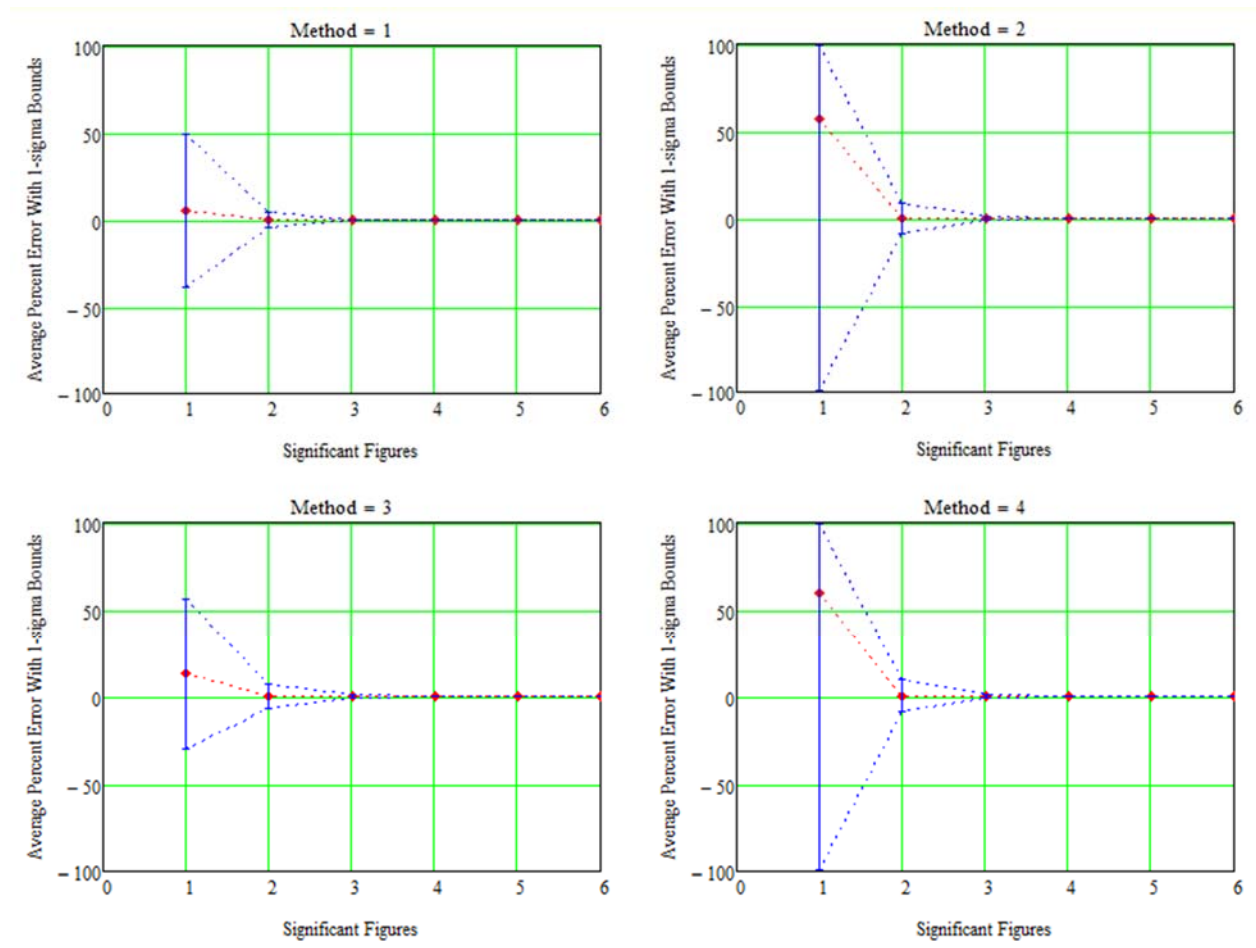


Fig. A1 Collision-probability calculation error using the four methods ( $OBJ \leq d$ ,  $AR=1$ ).

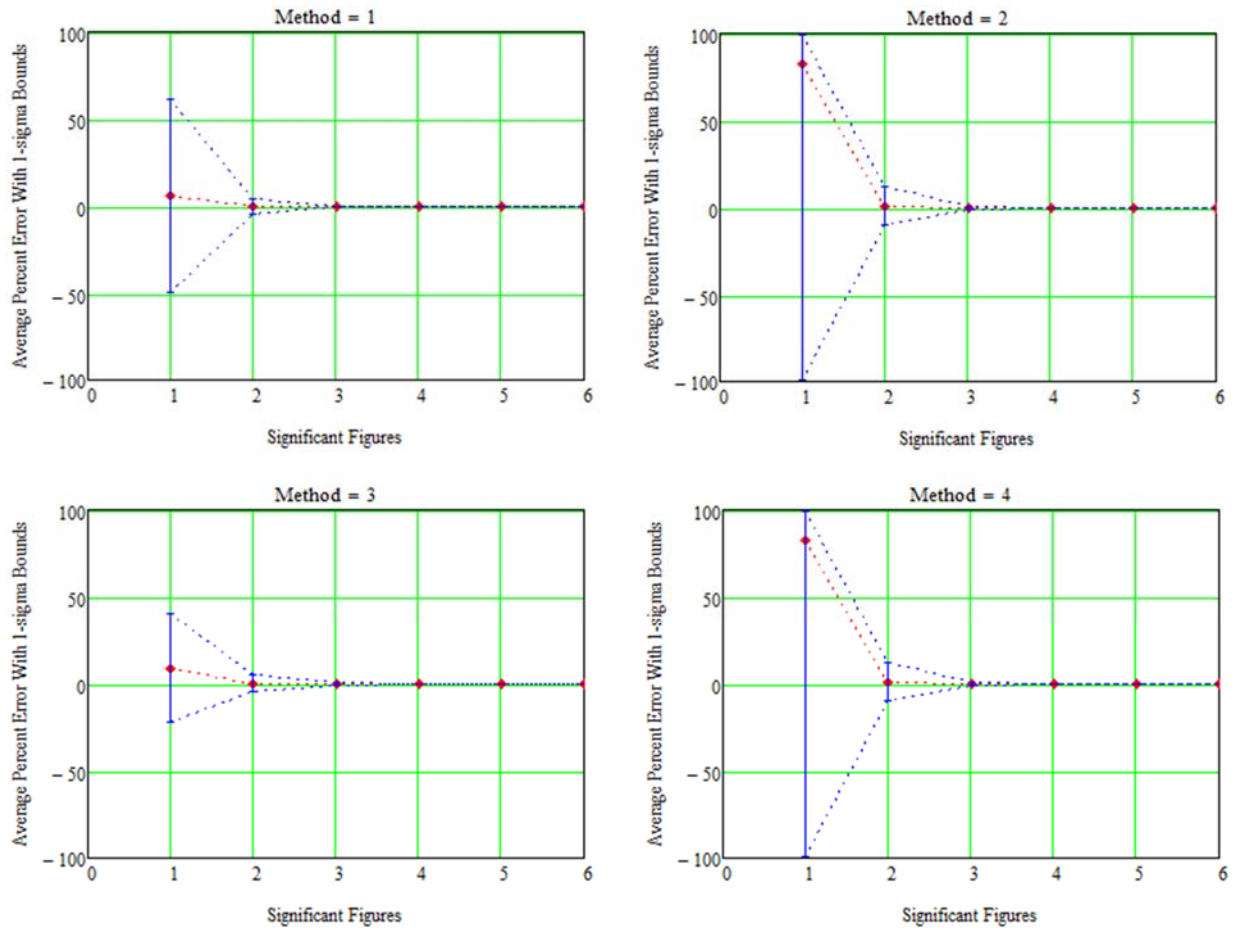


Fig. A2 Collision-probability calculation error using the four methods ( $OBJ \leq d$ ,  $AR=2$ ).

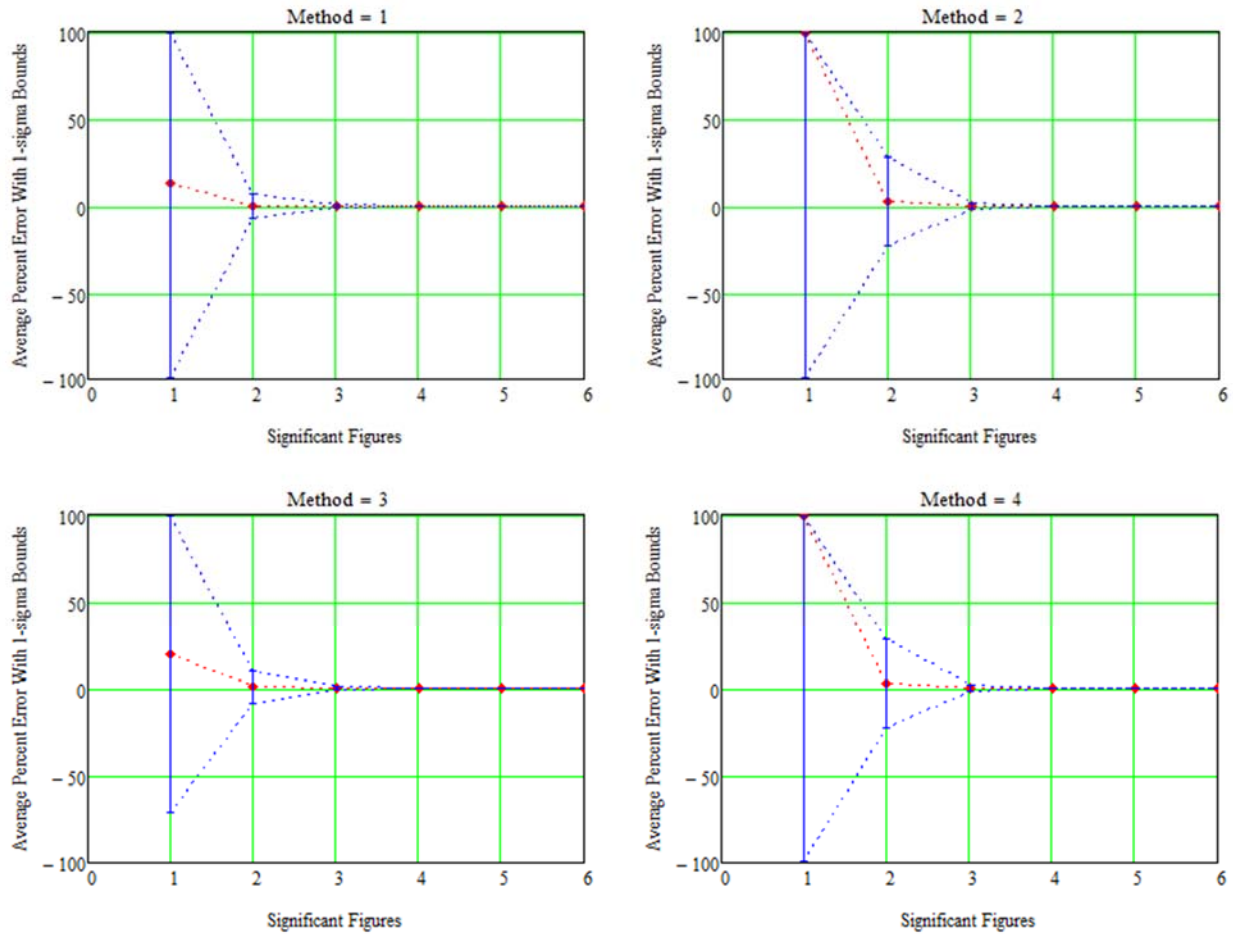


Fig. A3 Collision-probability calculation error using the four methods ( $OBJ \leq d$ ,  $AR=3$ ).

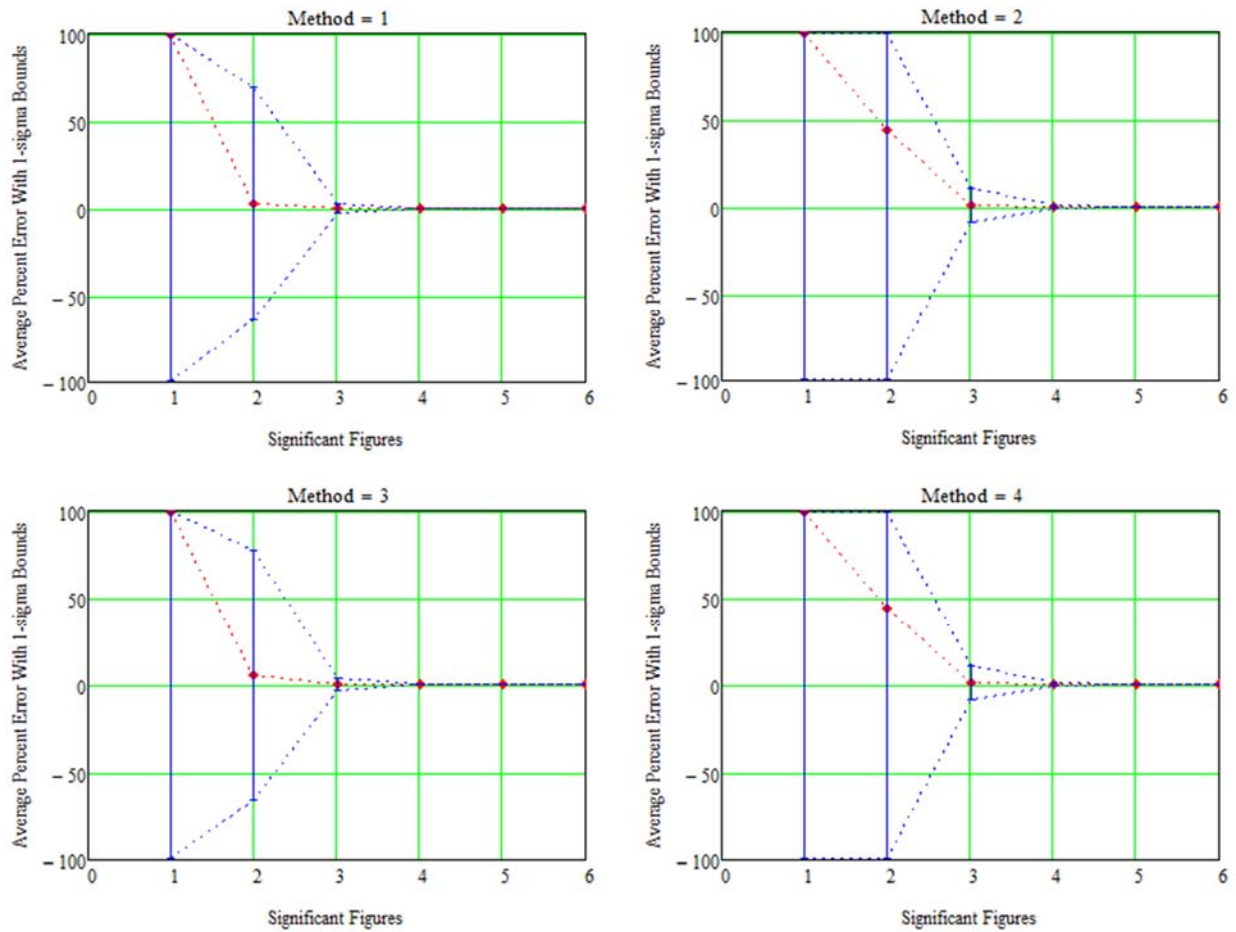


Fig. A4 Collision-probability calculation error using the four methods ( $OBJ \leq d$ ,  $AR=5$ ).

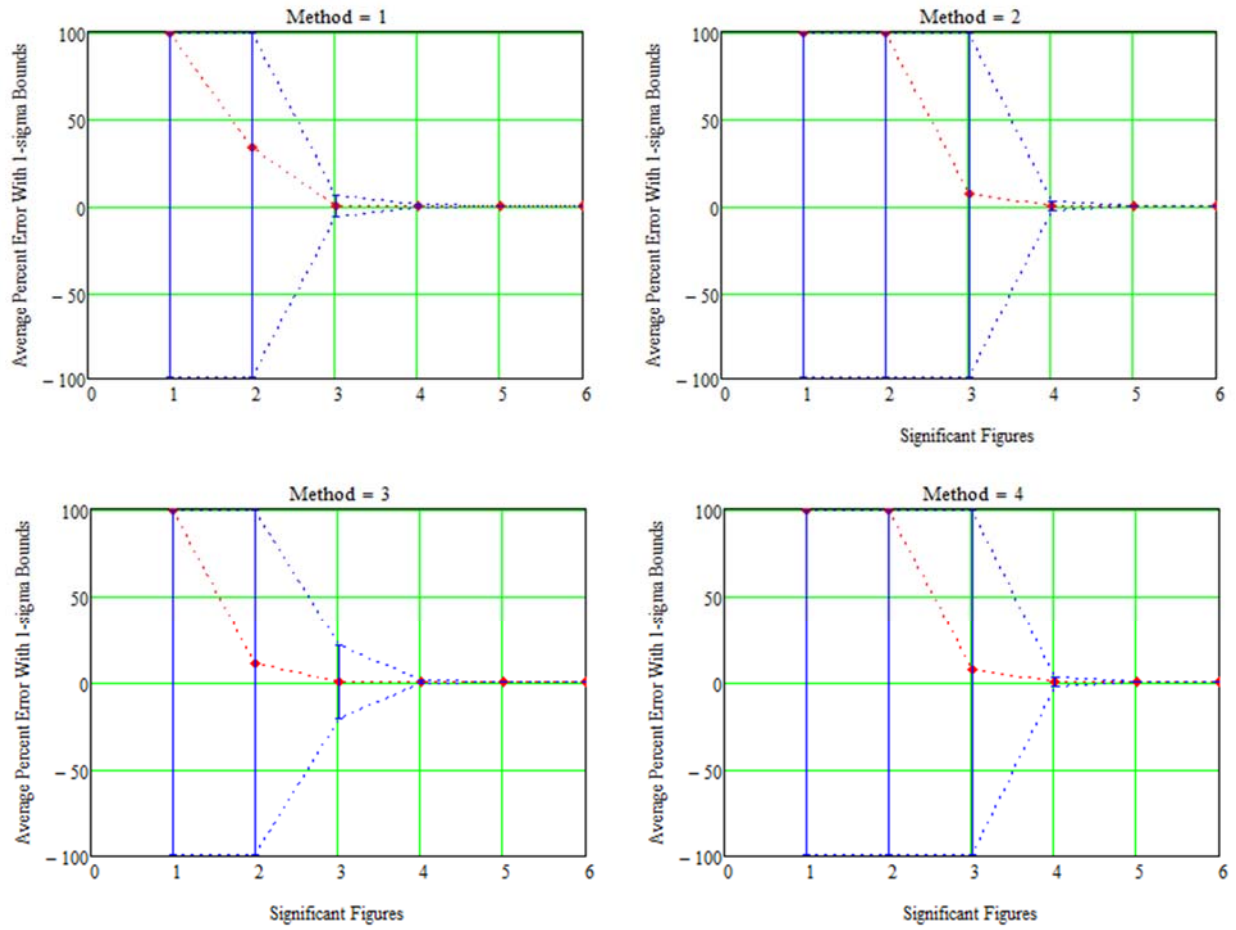
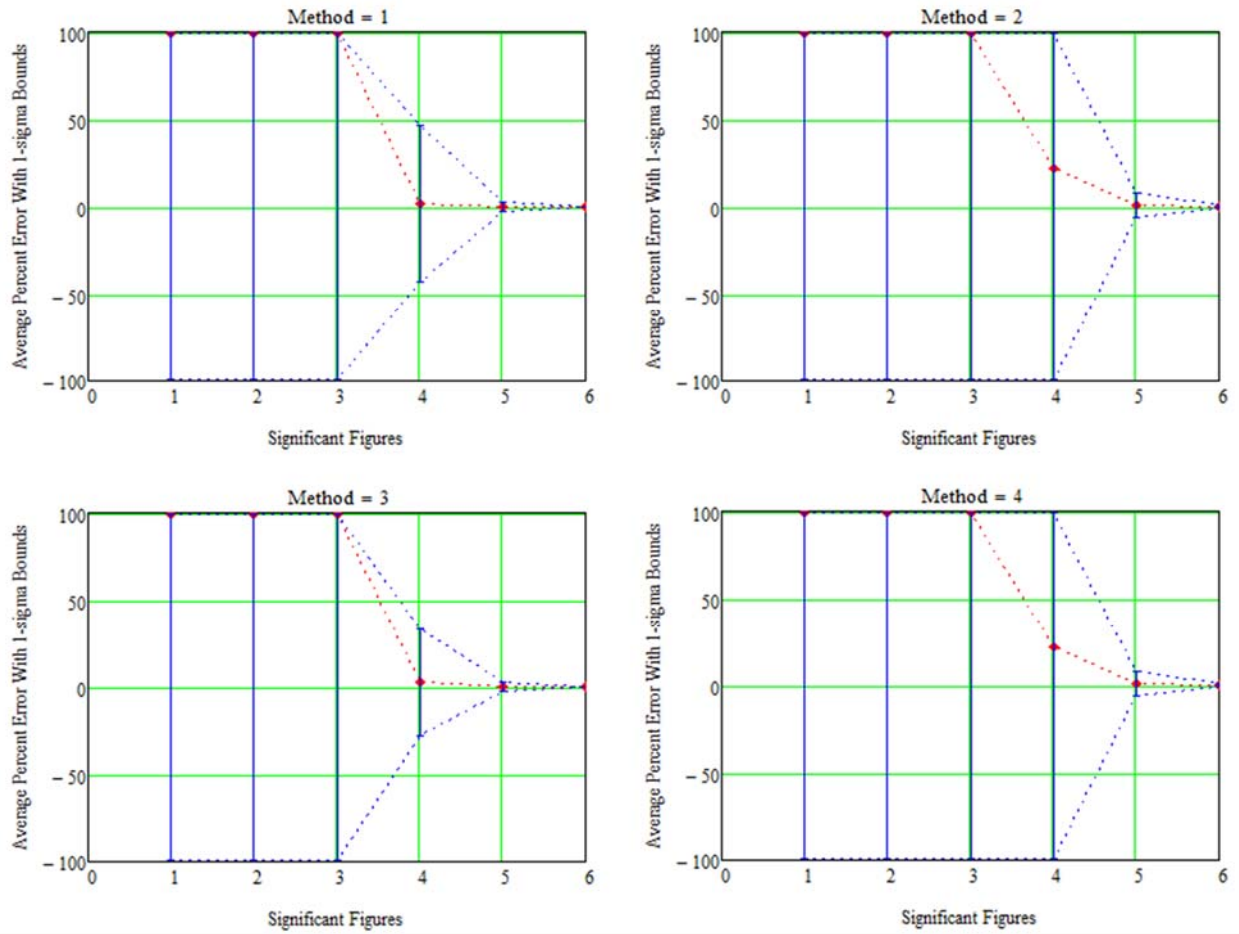
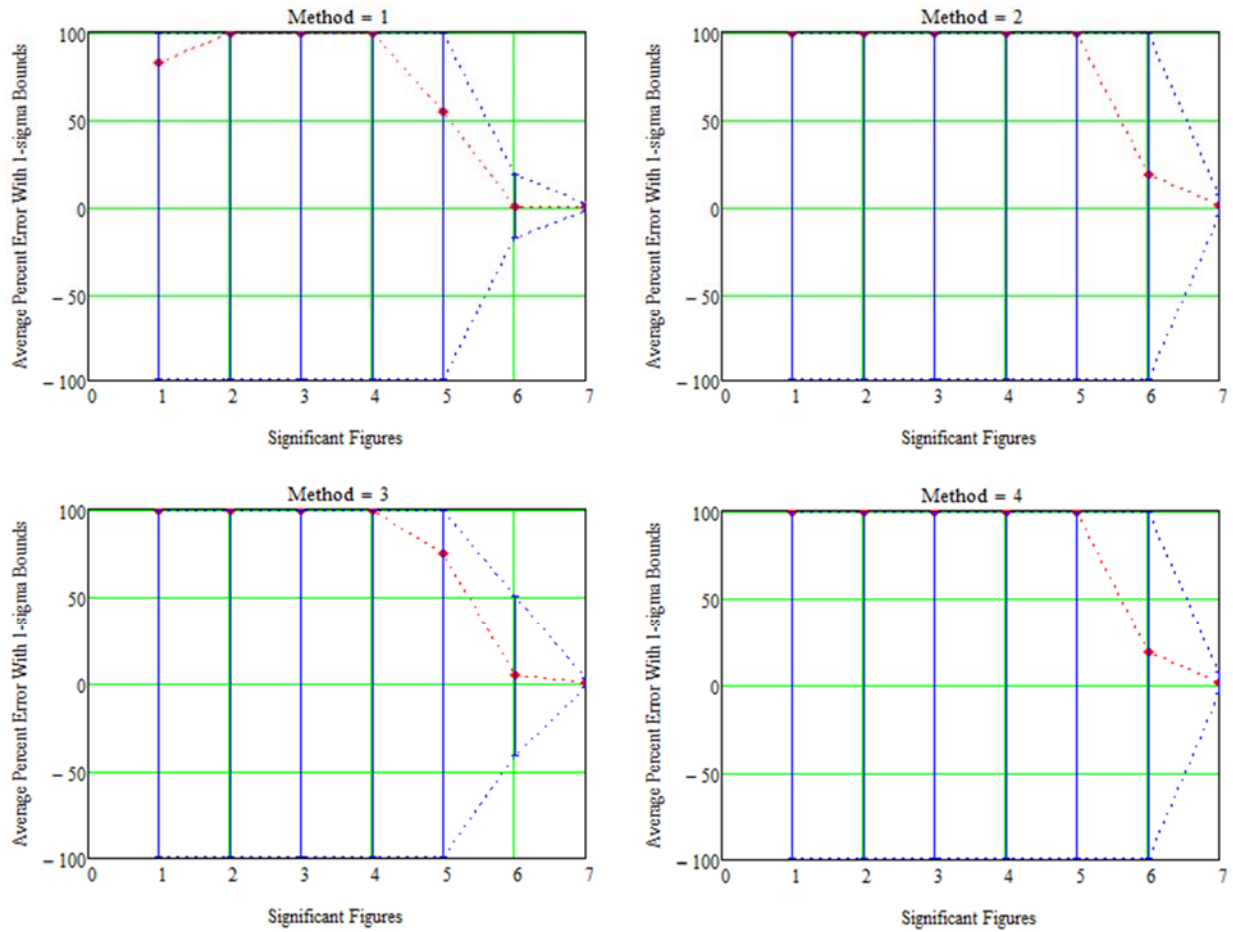


Fig. A5 Collision-probability calculation error using the four methods ( $OBJ \leq d$ ,  $AR=10$ ).



**Fig. A6** Collision-probability calculation error using the four methods ( $OBJ \leq d$ ,  $AR=50$ ).



**Fig. A7** Collision-probability calculation error using the four methods ( $OBJ \leq d$ ,  $AR=500$ ).

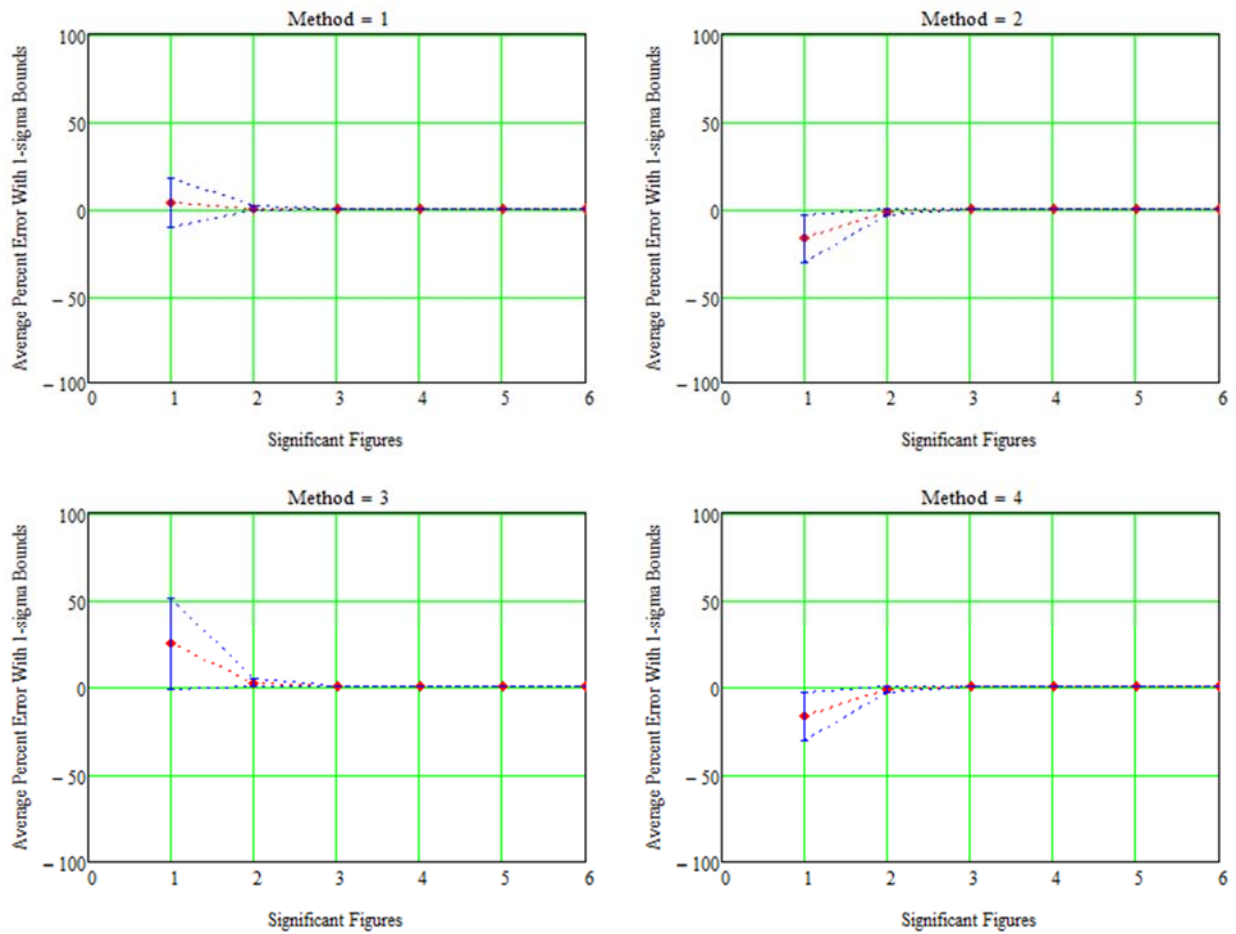


**Fig. A8** Collision-probability calculation error using the four methods ( $OBJ > d$ ,  $AR=1$ ).

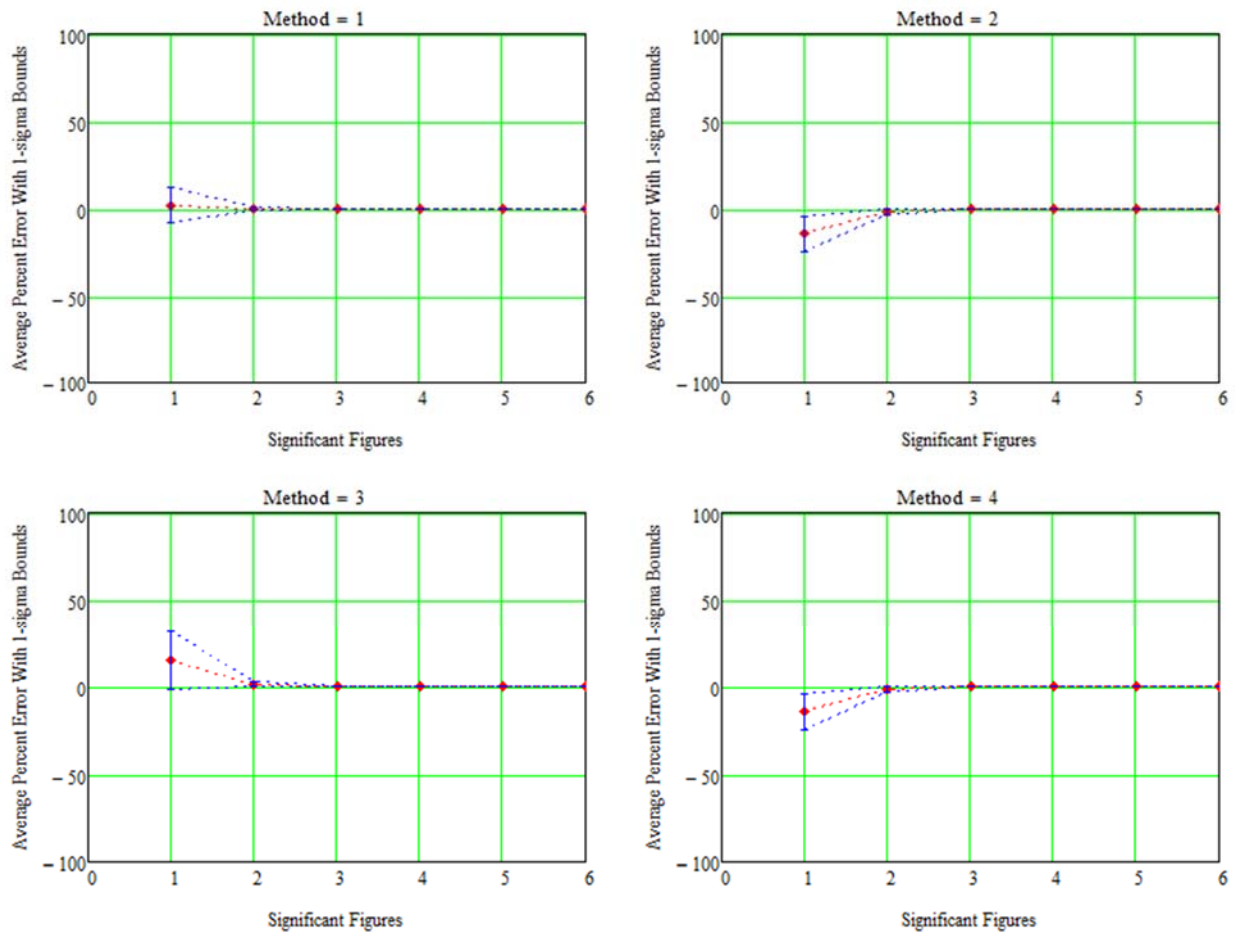


**Fig. A9** Collision-probability calculation error using the four methods ( $OBJ > d$ ,  $AR=2$ ).

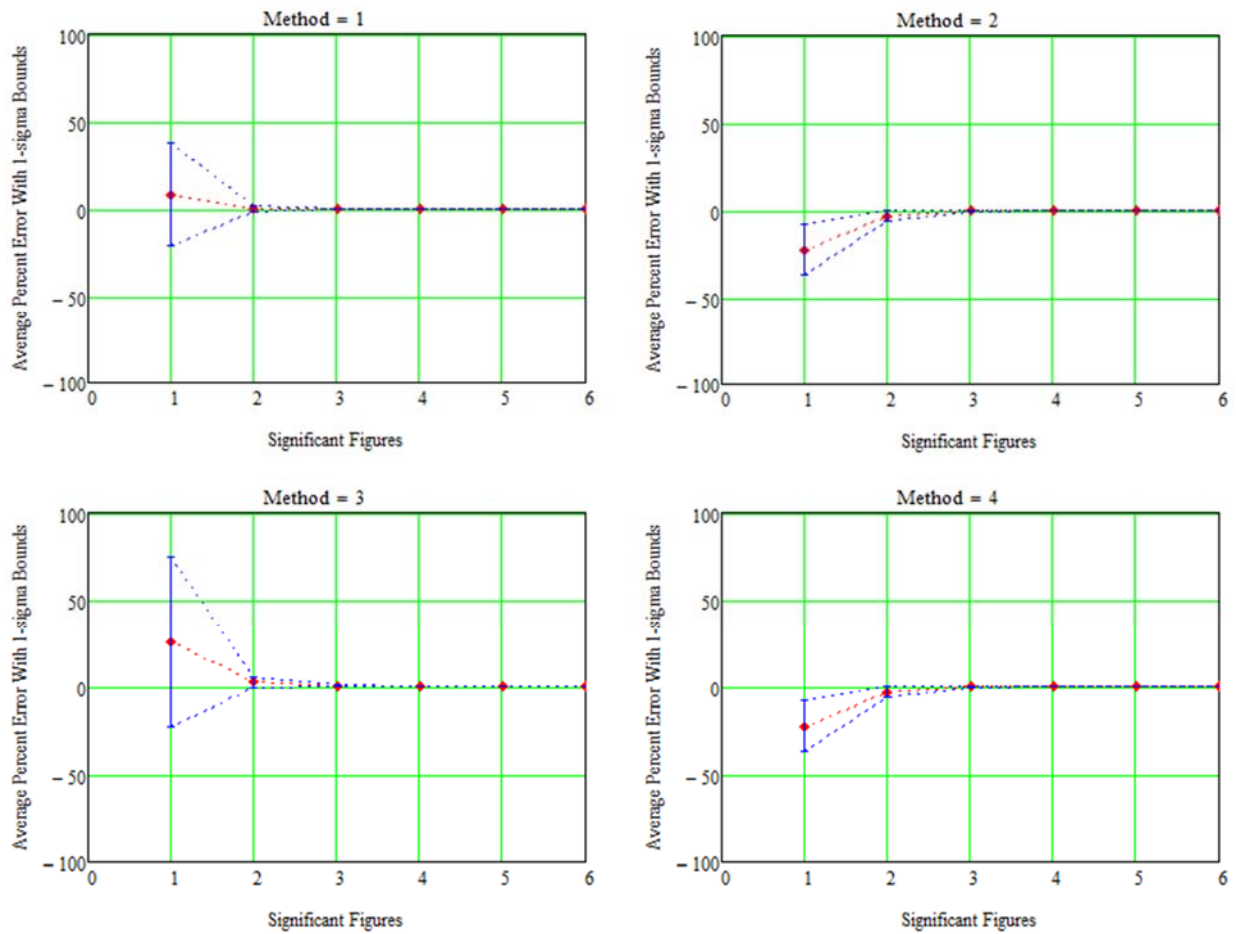


Fig. A10 Collision-probability calculation error using the four methods ( $OBJ > d$ ,  $AR=3$ ).

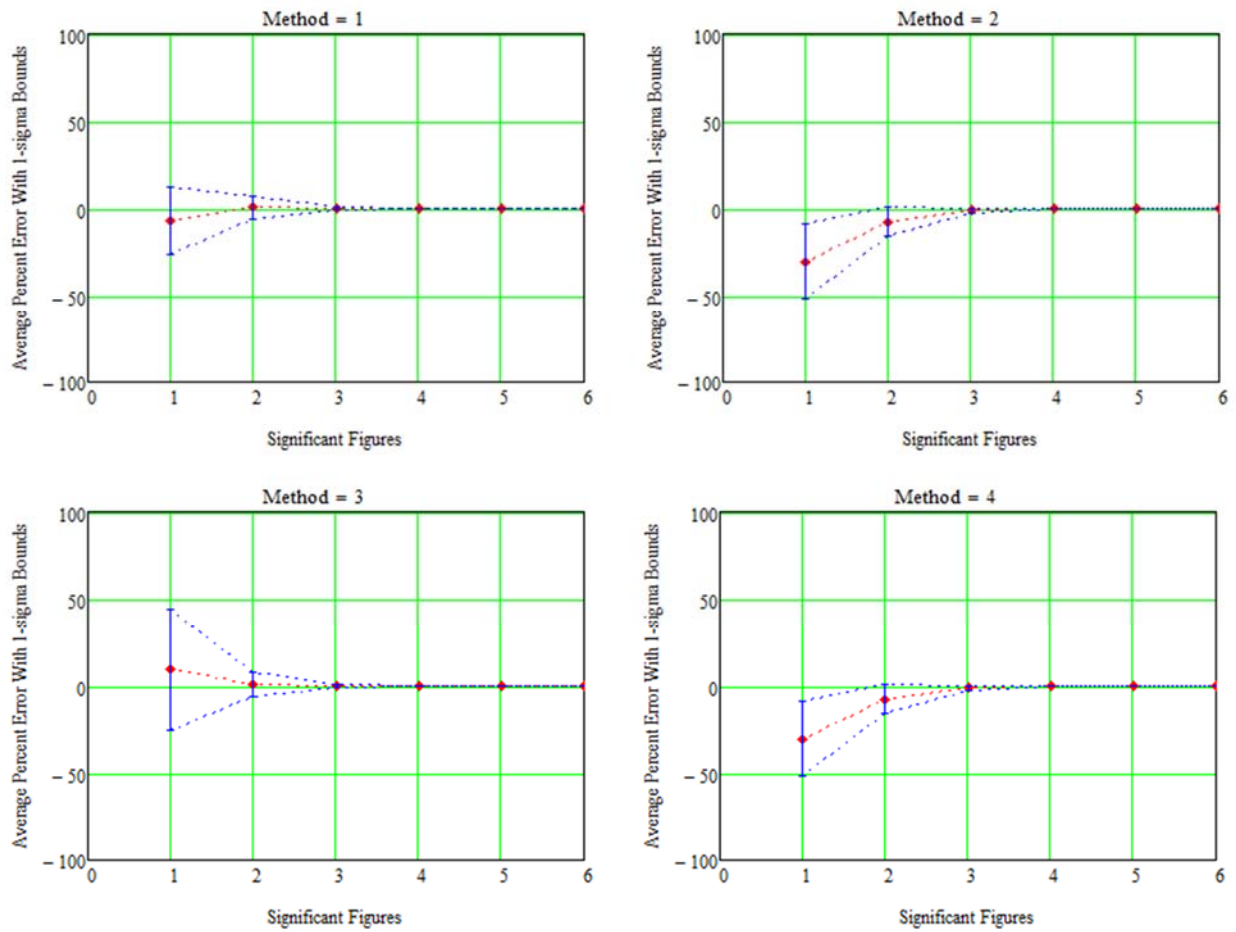


Fig. A11 Collision-probability calculation error using the four methods ( $OBJ > d$ ,  $AR=5$ ).

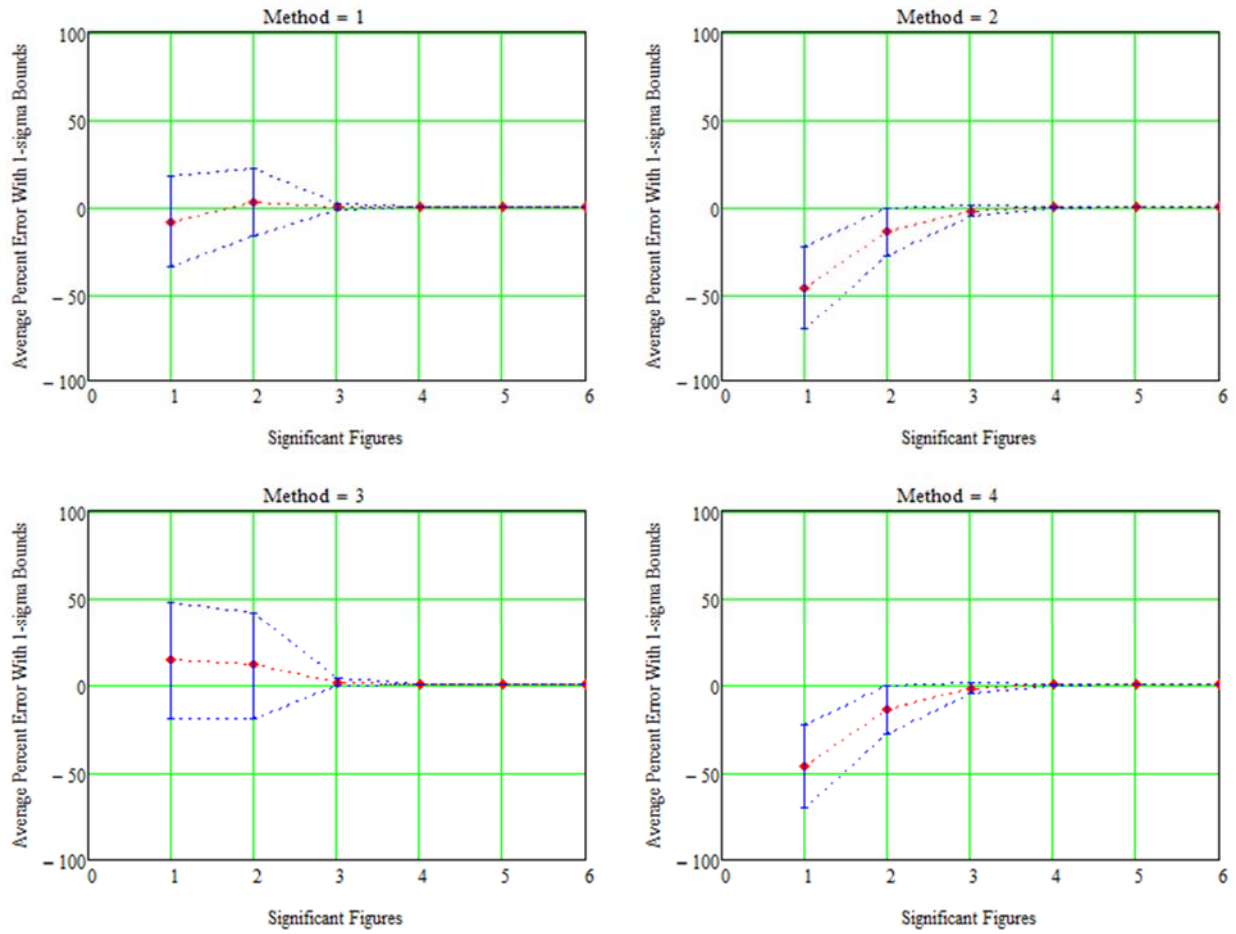


Fig. A12 Collision-probability calculation error using the four methods ( $OBJ > d$ ,  $AR=10$ ).

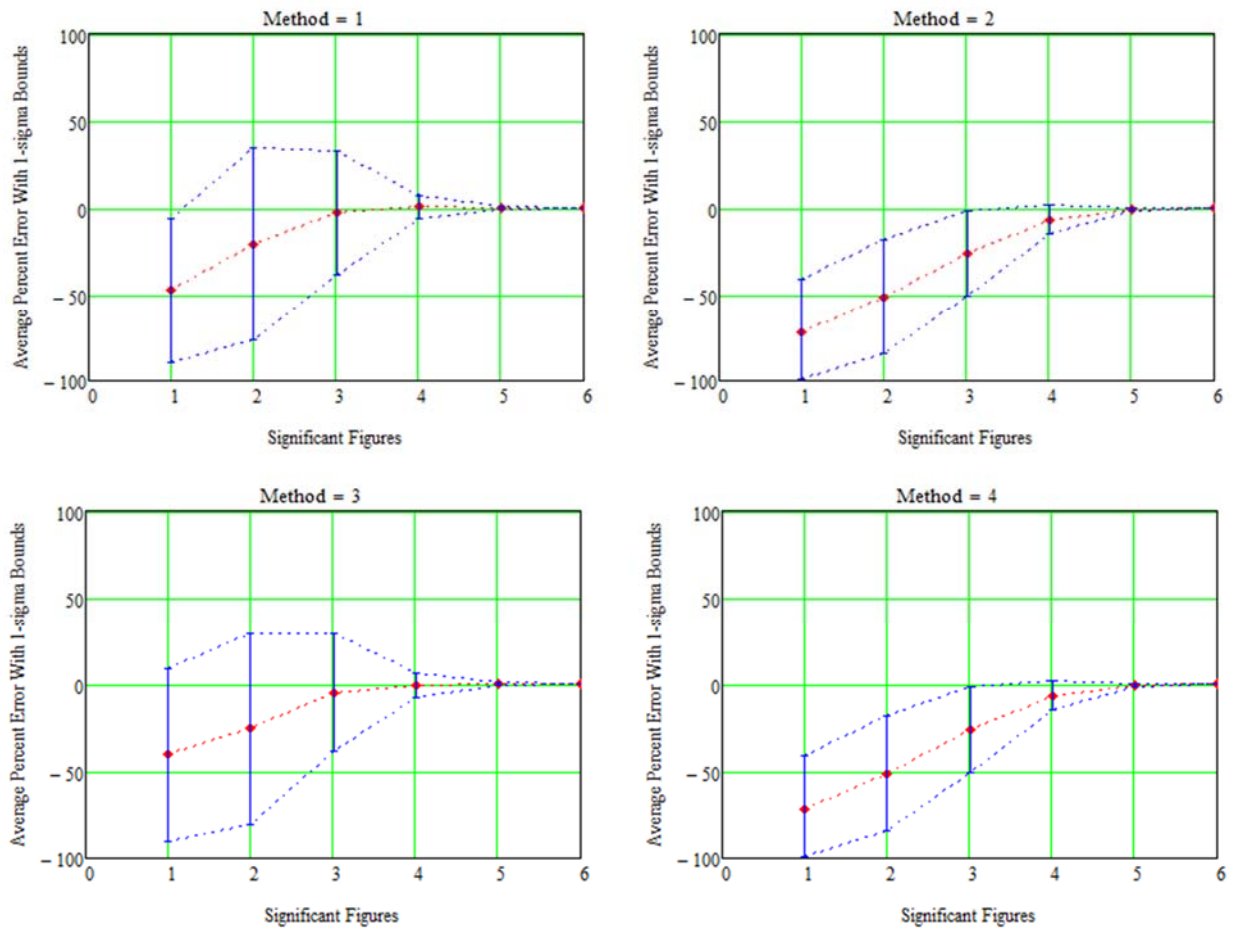


Fig. A13 Collision-probability calculation error using the four methods ( $OBJ > d$ ,  $AR=50$ ).

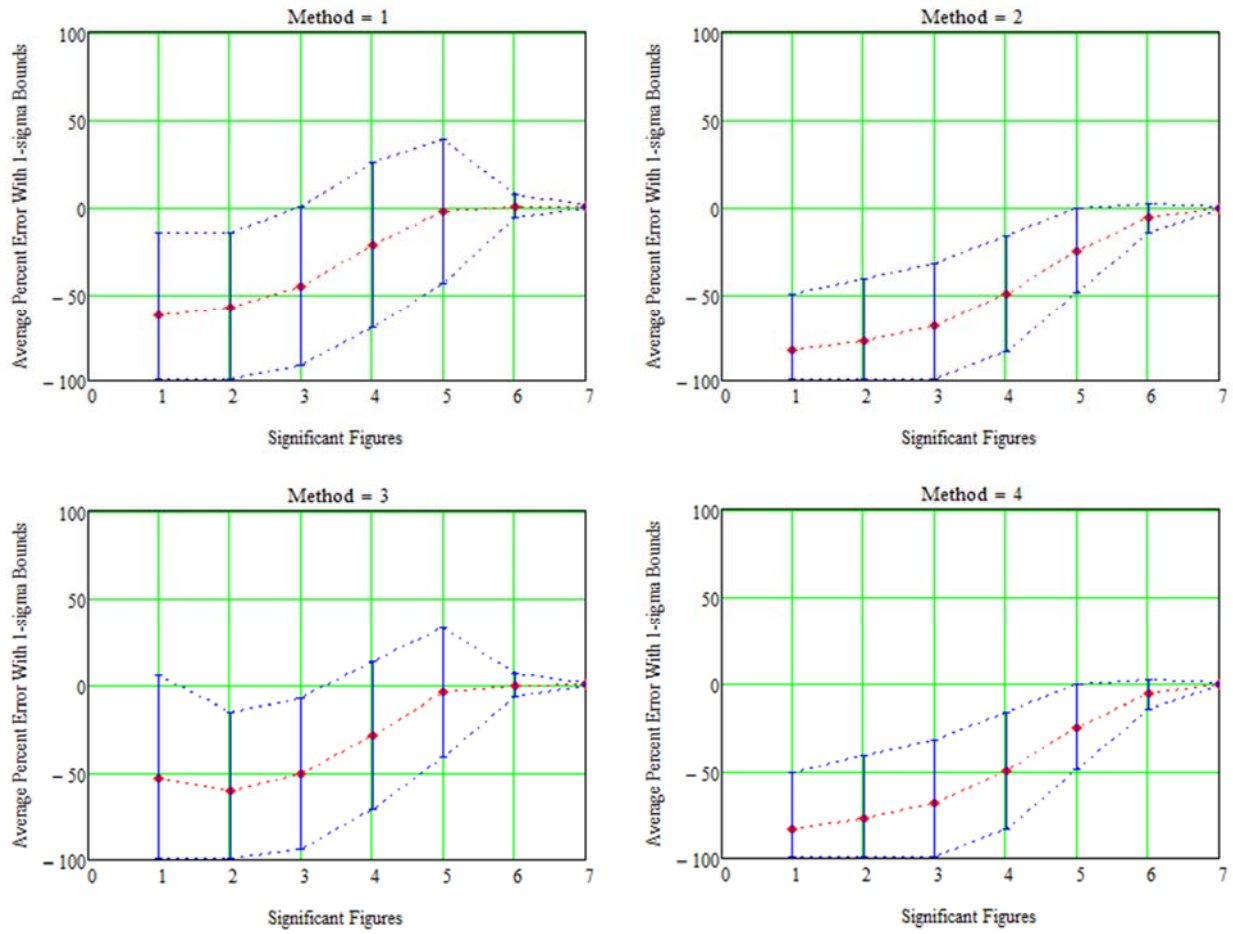


Fig. A14 Collision-probability calculation error using the four methods ( $OBJ > d$ ,  $AR = 500$ ).

## Appendix B

The following figures show the effects of significant figure reduction on collision probability calculations using all four methods for collision probabilities of  $10^{-7}$  or greater:

- 1) rounding all elements,
- 2) rounding up all elements,
- 3) truncating all elements, and
- 4) the hybrid approach (rounds up diagonal elements and truncates off-diagonal elements)).

After the methods were applied, the matrices that were no longer positive definite were remediated using the Eigenvalue Clipping Method. Relative percent errors of all covariance matrices (remediated and those that remained positive definite) are depicted in red. The error's one-sigma standard deviation is shown in blue. To make the plots more readable, all plots have the error data clipped at 100%.

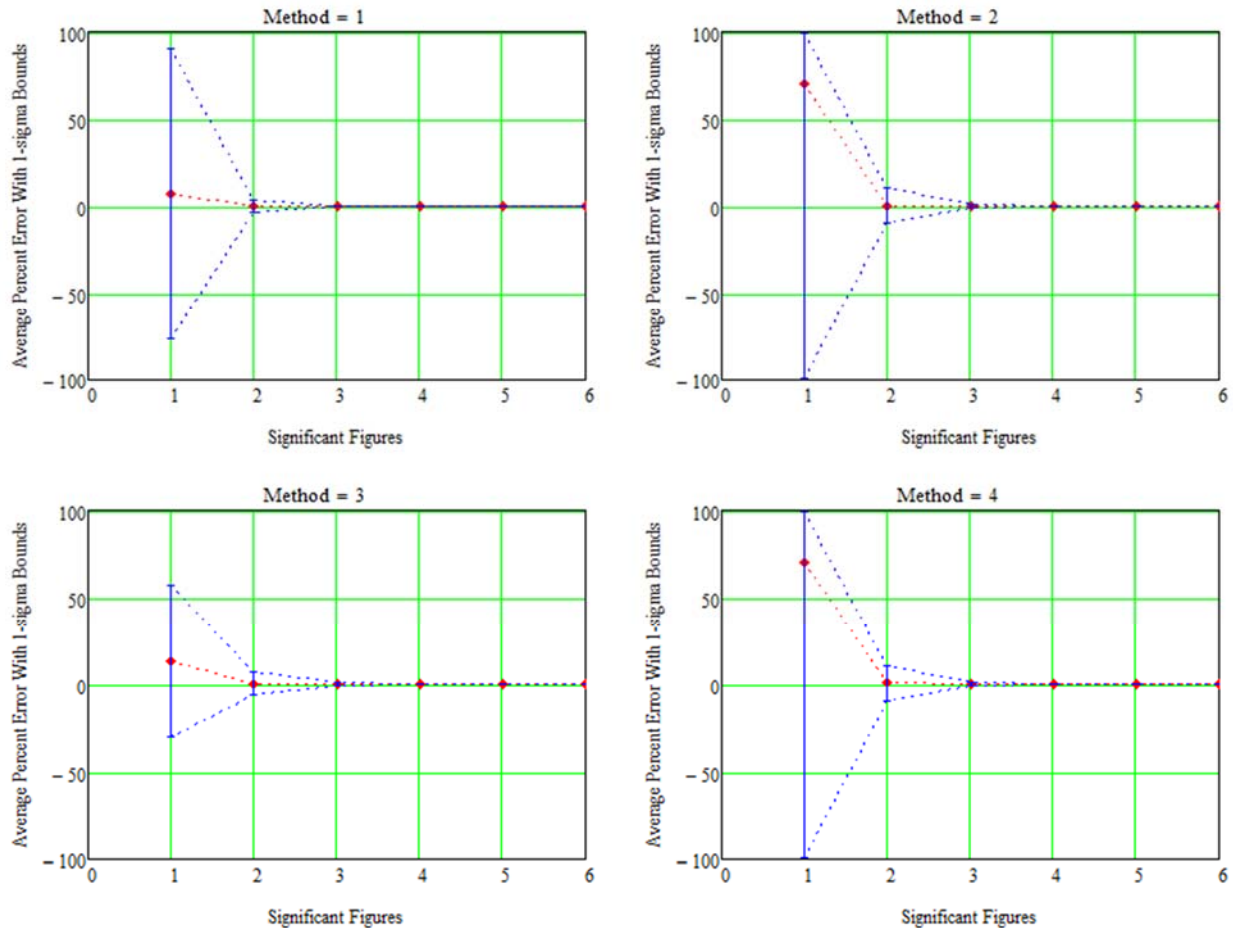
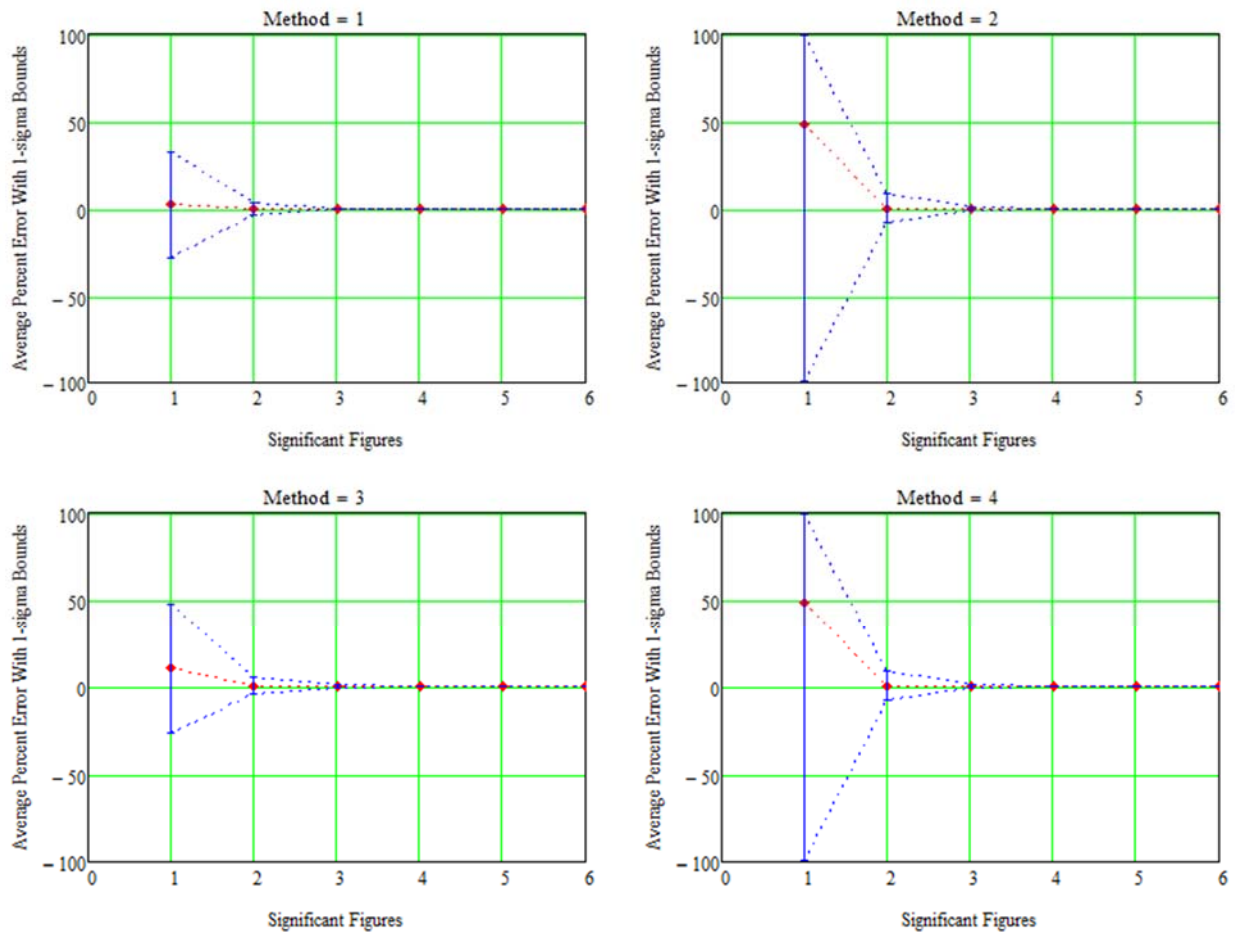


Fig. 1 Collision-probability calculation error using the four methods ( $OBJ \leq d$ ,  $AR=1$ ).



**Fig. 2 Collision-probability calculation error using the four methods ( $OBJ \leq d$ ,  $AR=2$ ).**

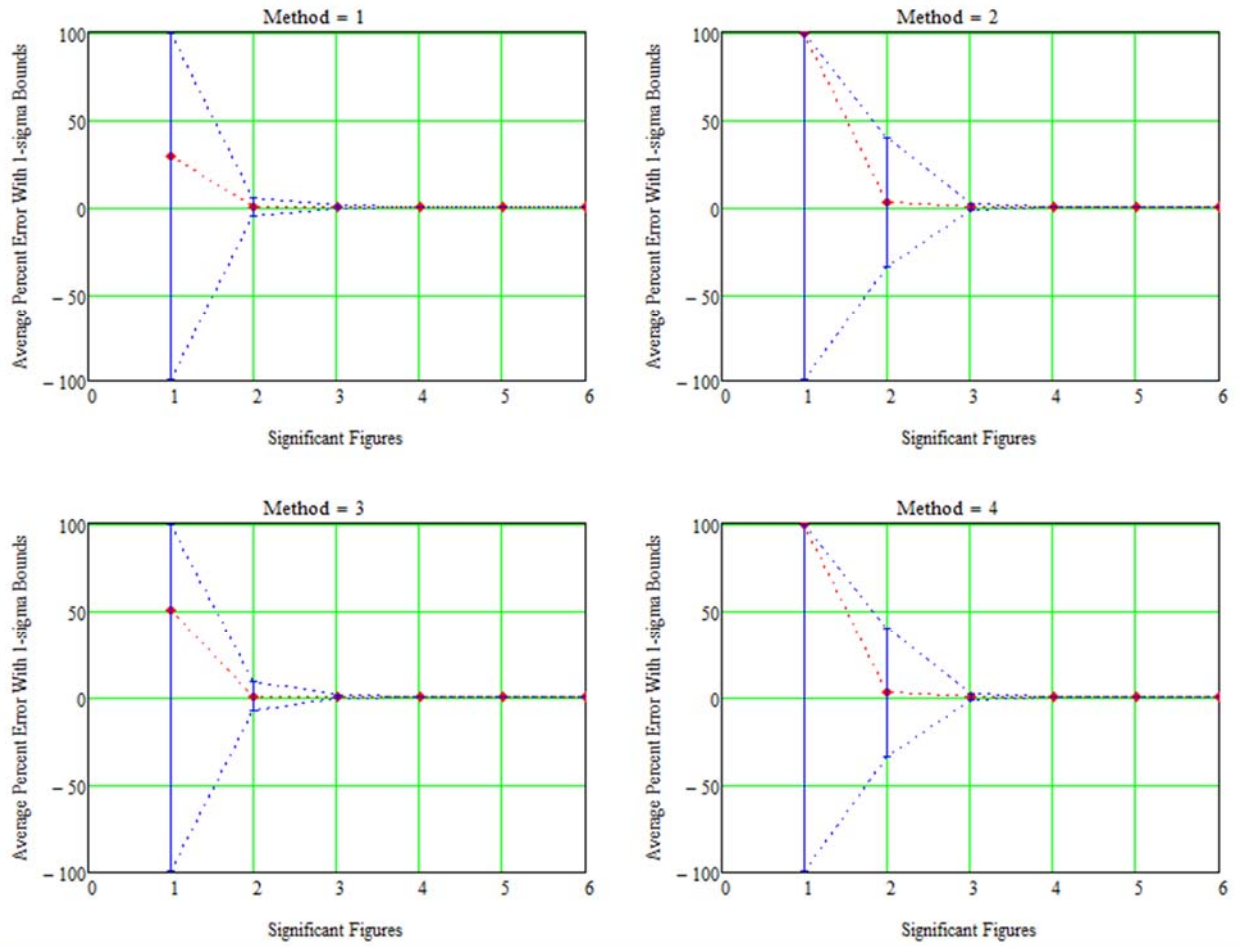


Fig. 3 Collision-probability calculation error using the four methods ( $OBJ \leq d$ ,  $AR=3$ ).

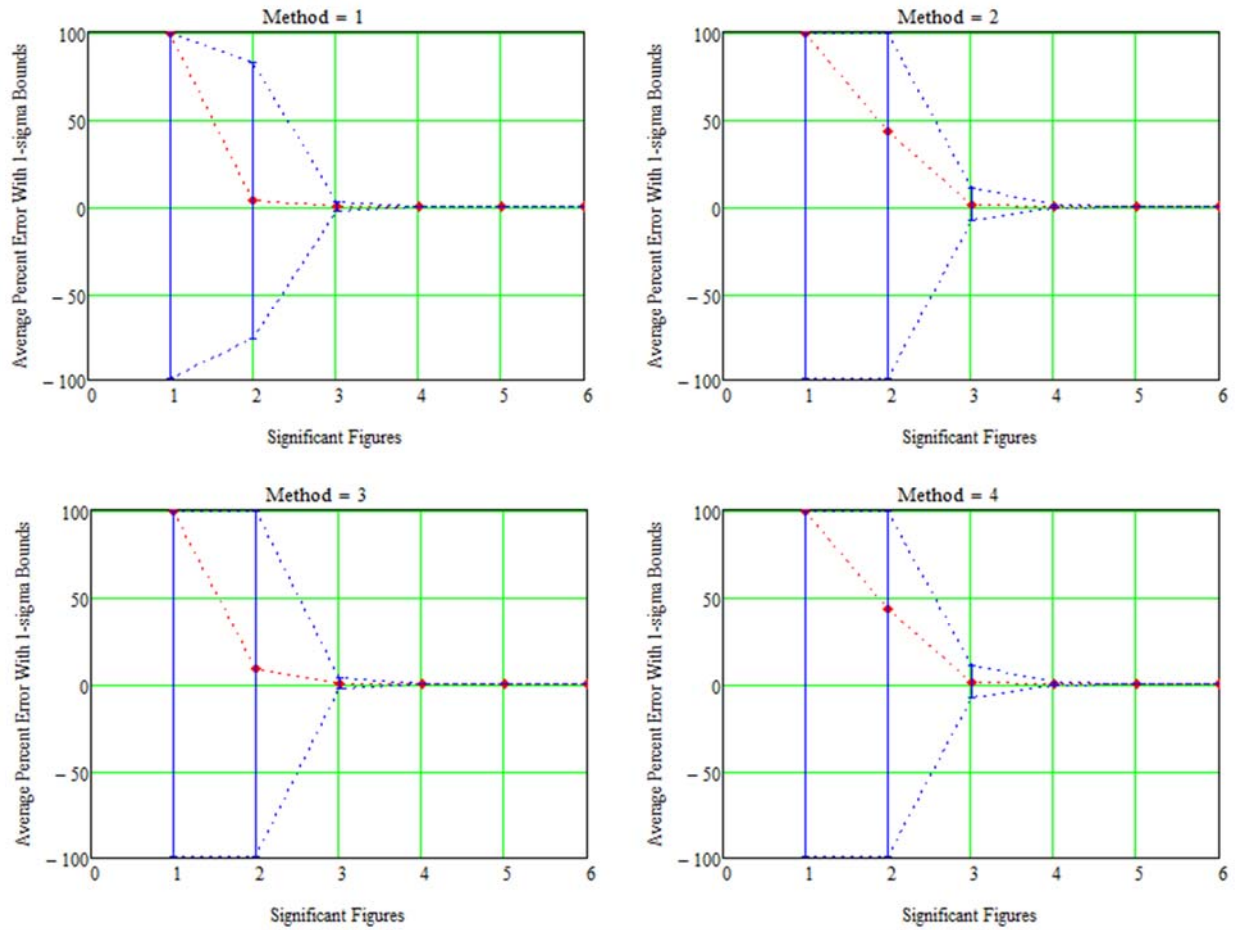
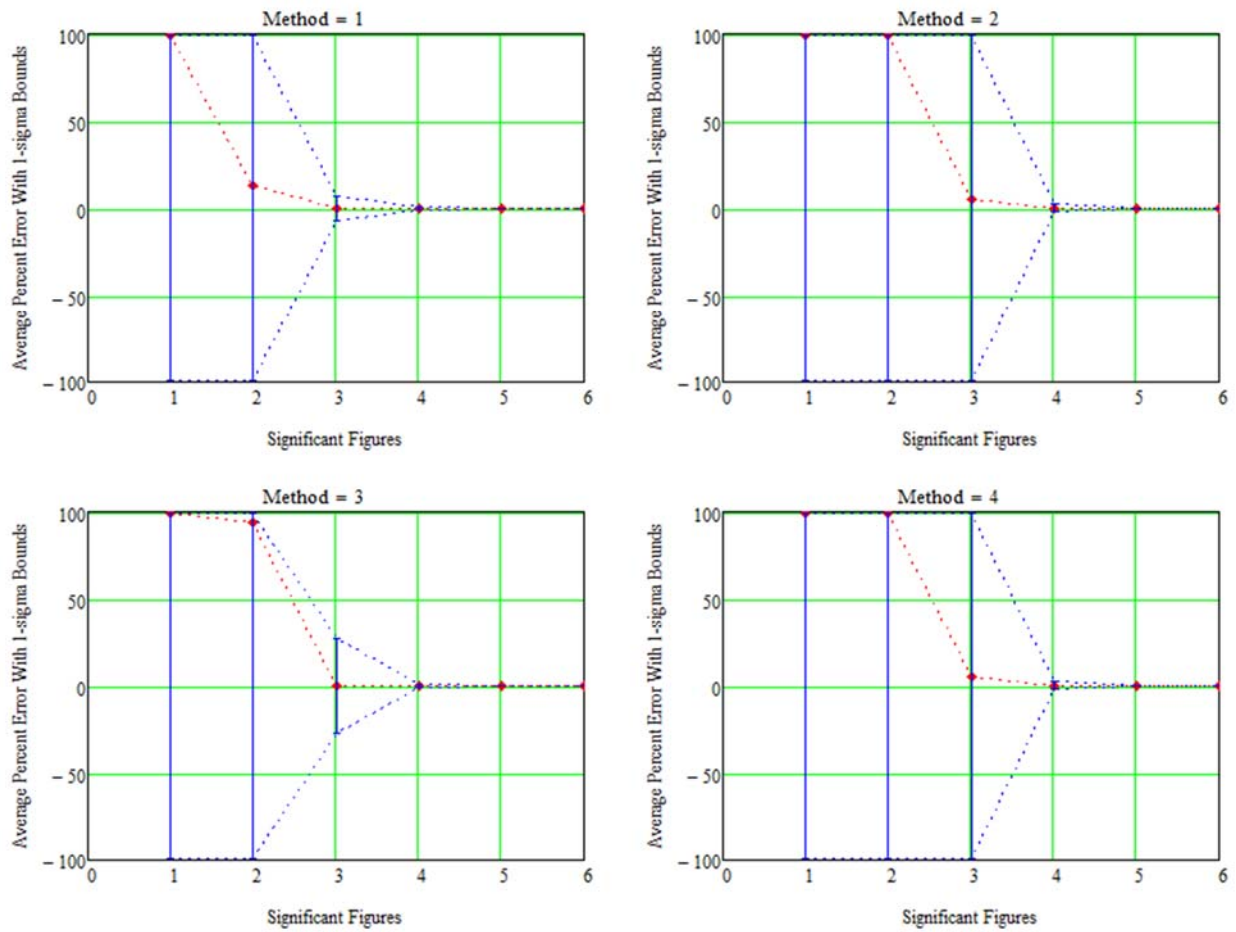
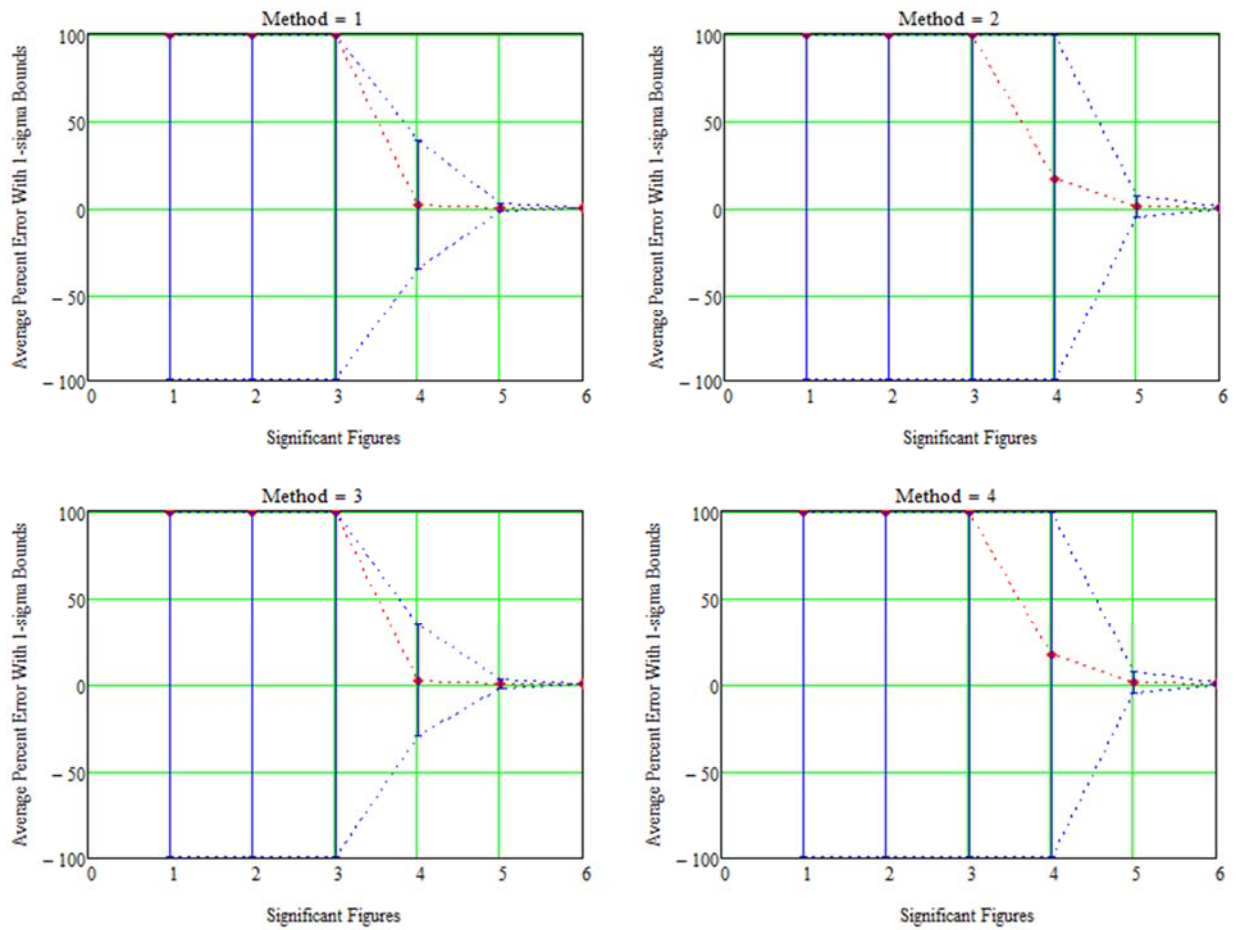


Fig. 4 Collision-probability calculation error using the four methods ( $OBJ \leq d$ ,  $AR=5$ ).



**Fig. 5** Collision-probability calculation error using the four methods ( $OBJ \leq d$ ,  $AR=10$ ).



**Fig. 6 Collision-probability calculation error using the four methods ( $OBJ \leq d$ ,  $AR=50$ ).**

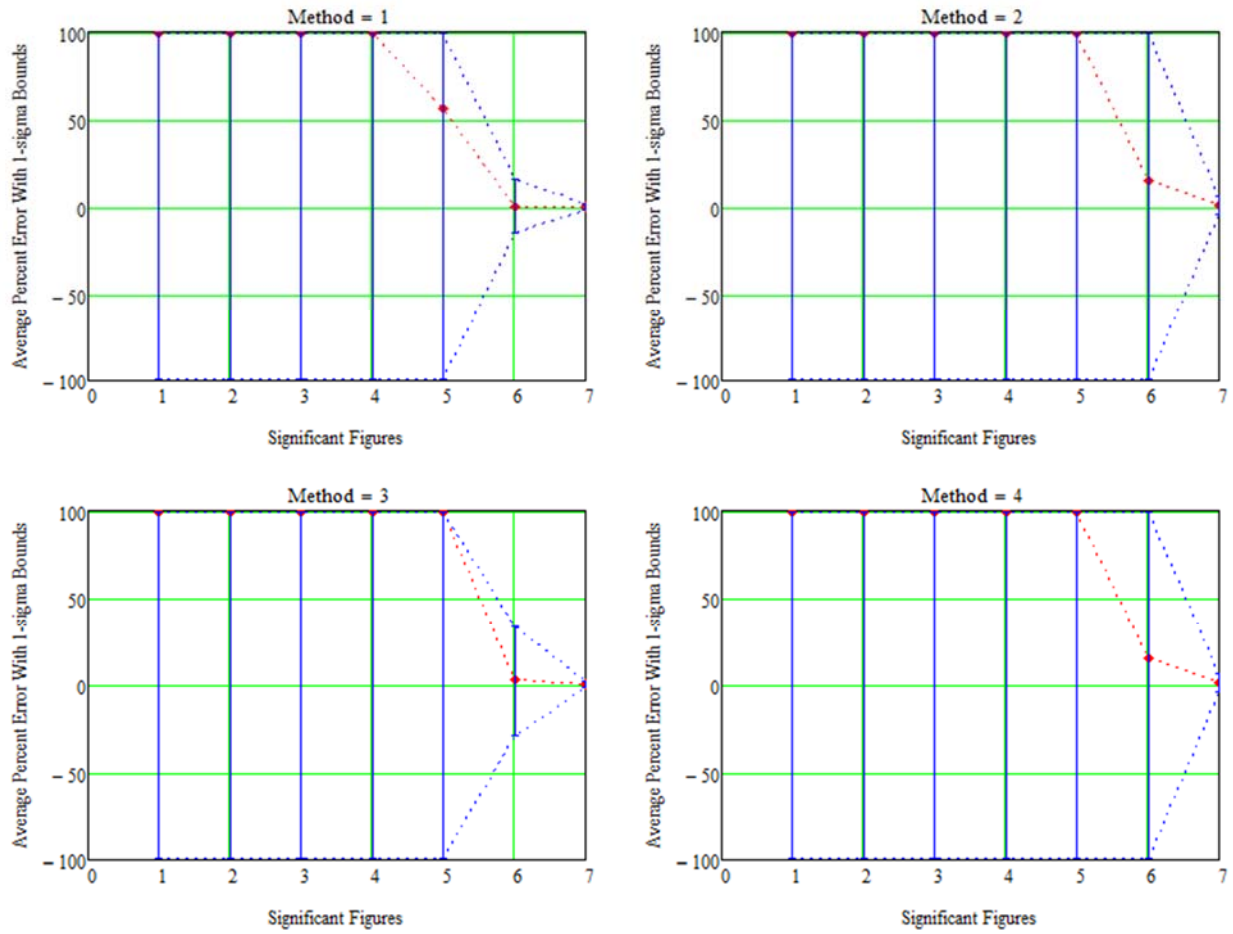


**Fig. 7 Collision-probability calculation error using the four methods ( $OBJ \leq d$ ,  $AR=500$ ).**

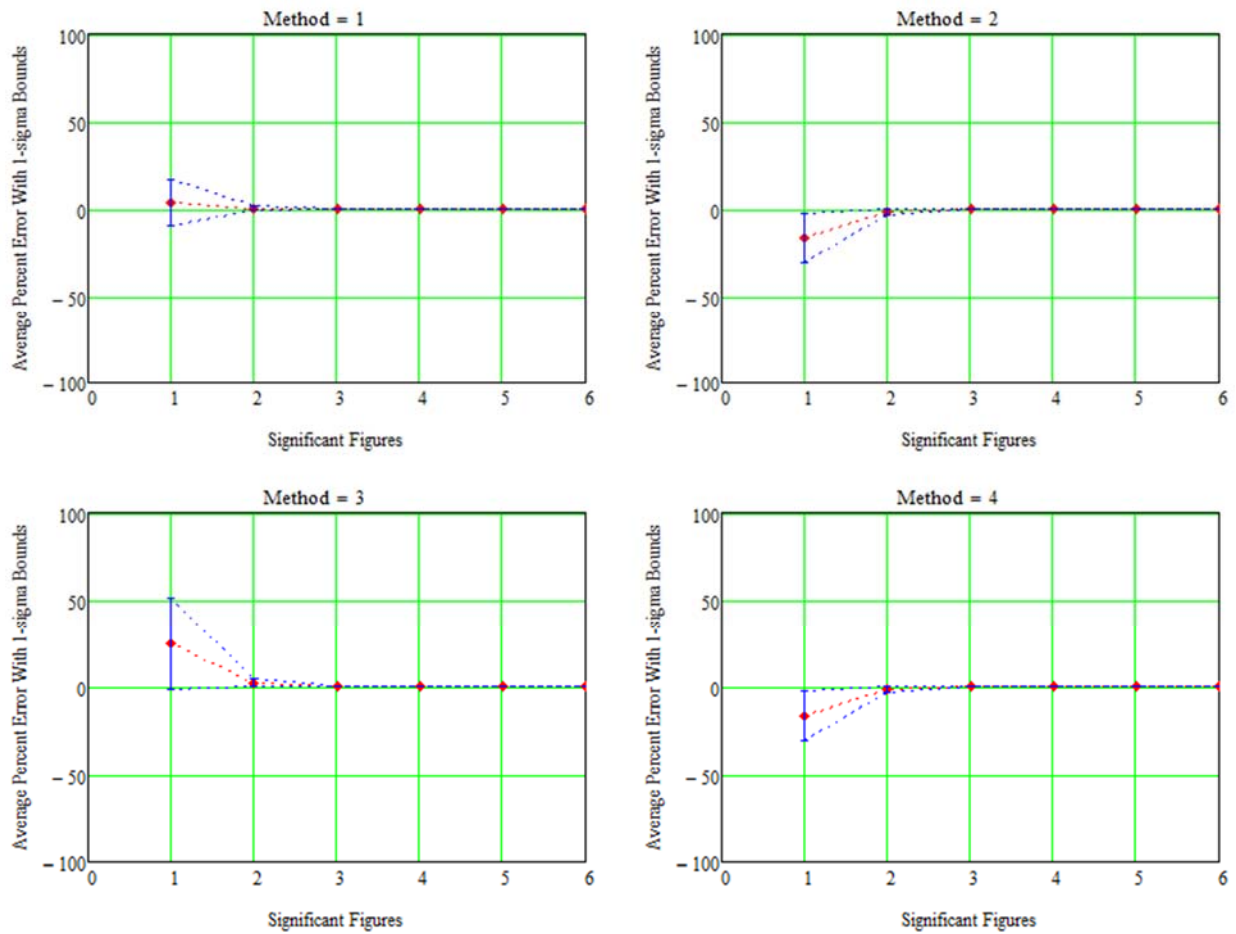


**Fig. 8** Collision-probability calculation error using the four methods ( $OBJ > d$ ,  $AR = 1$ ).

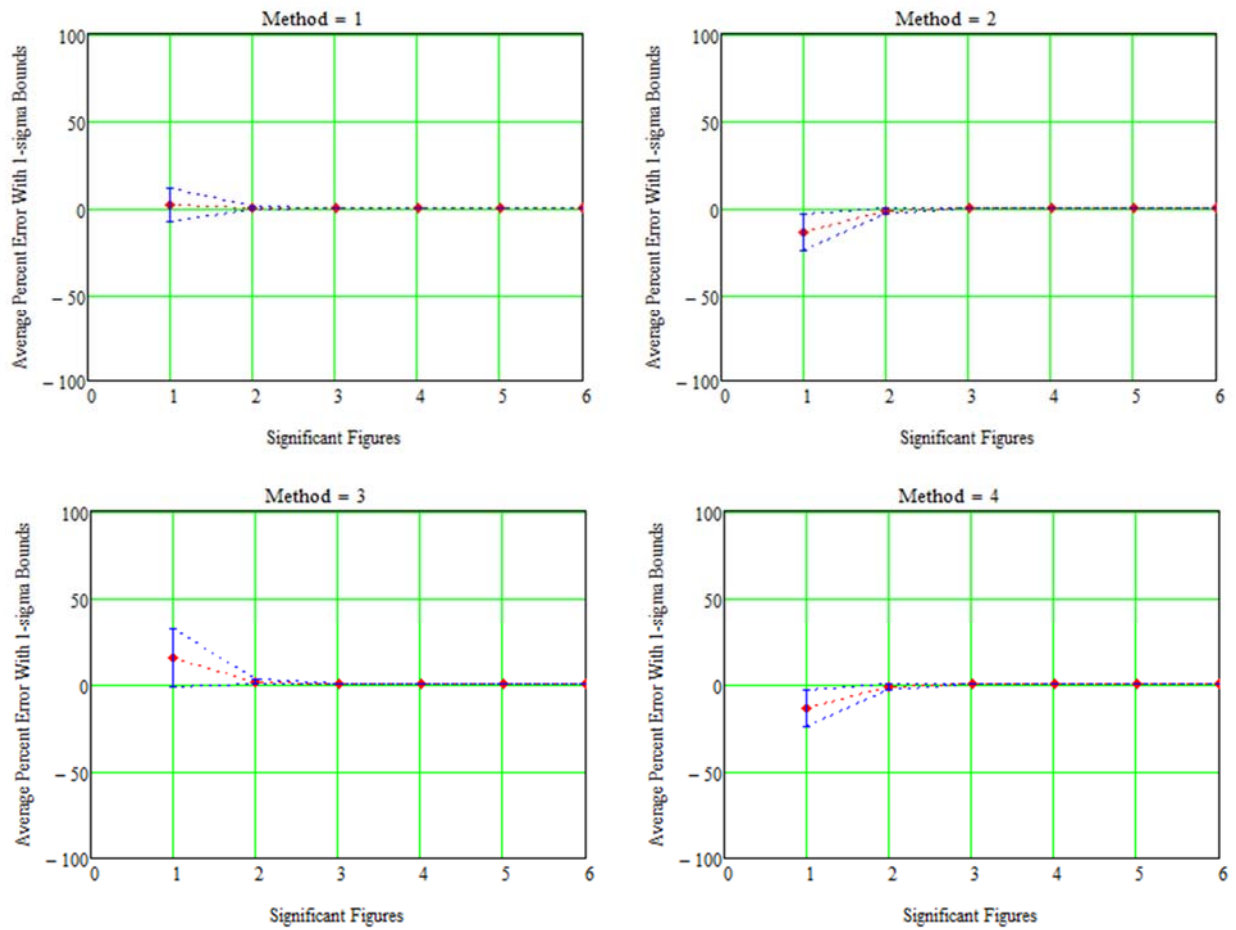


**Fig. 9** Collision-probability calculation error using the four methods ( $OBJ > d$ ,  $AR=2$ ).

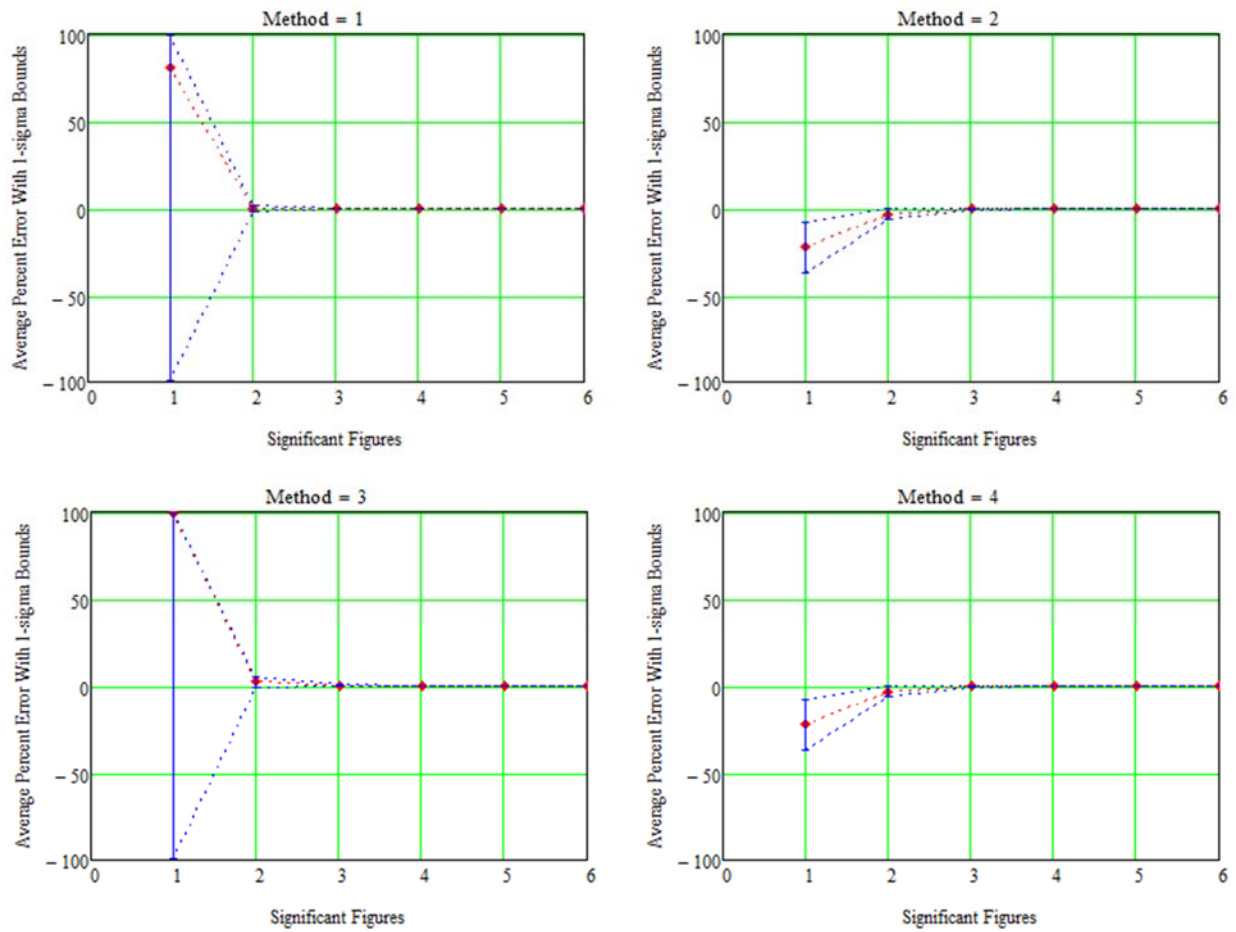
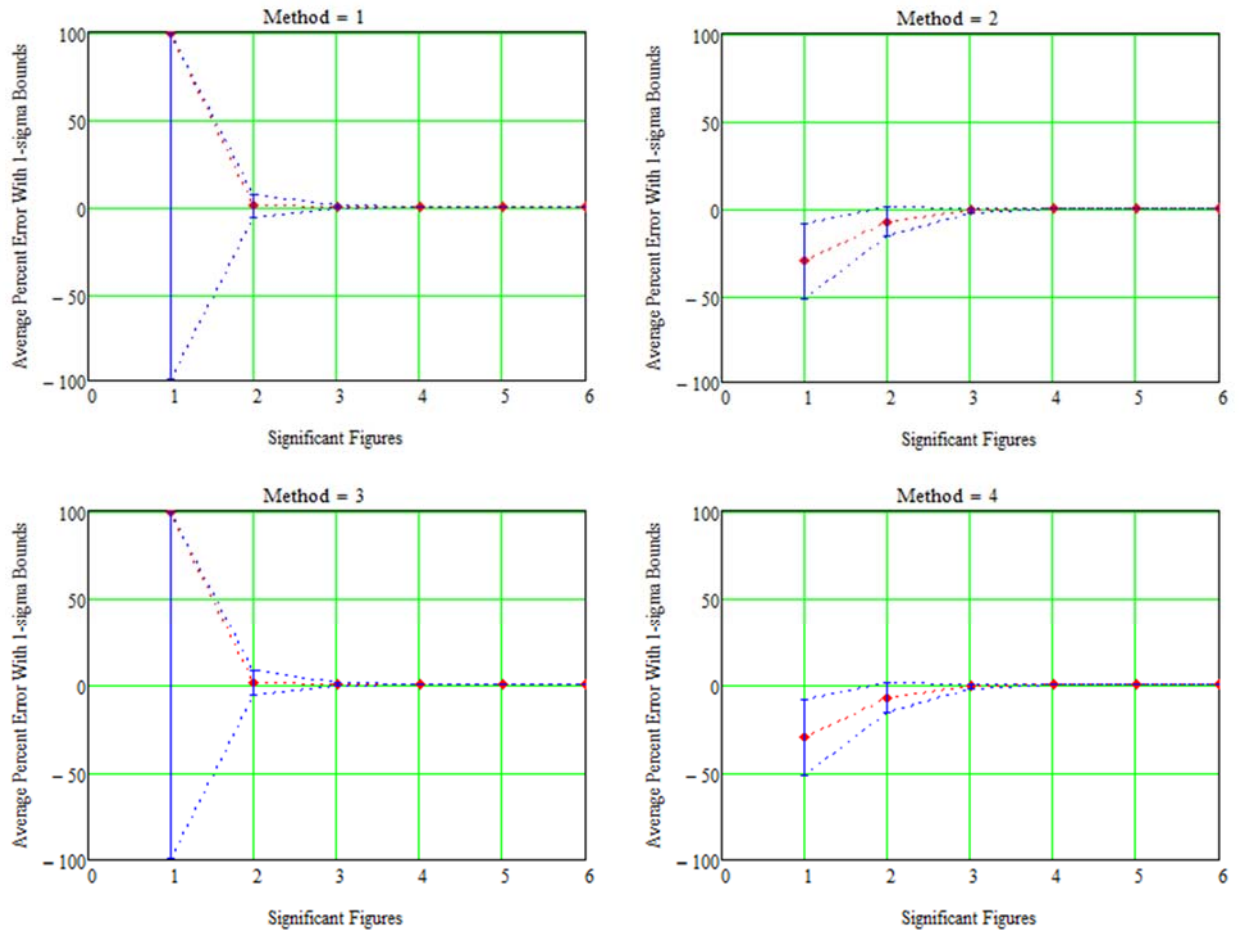
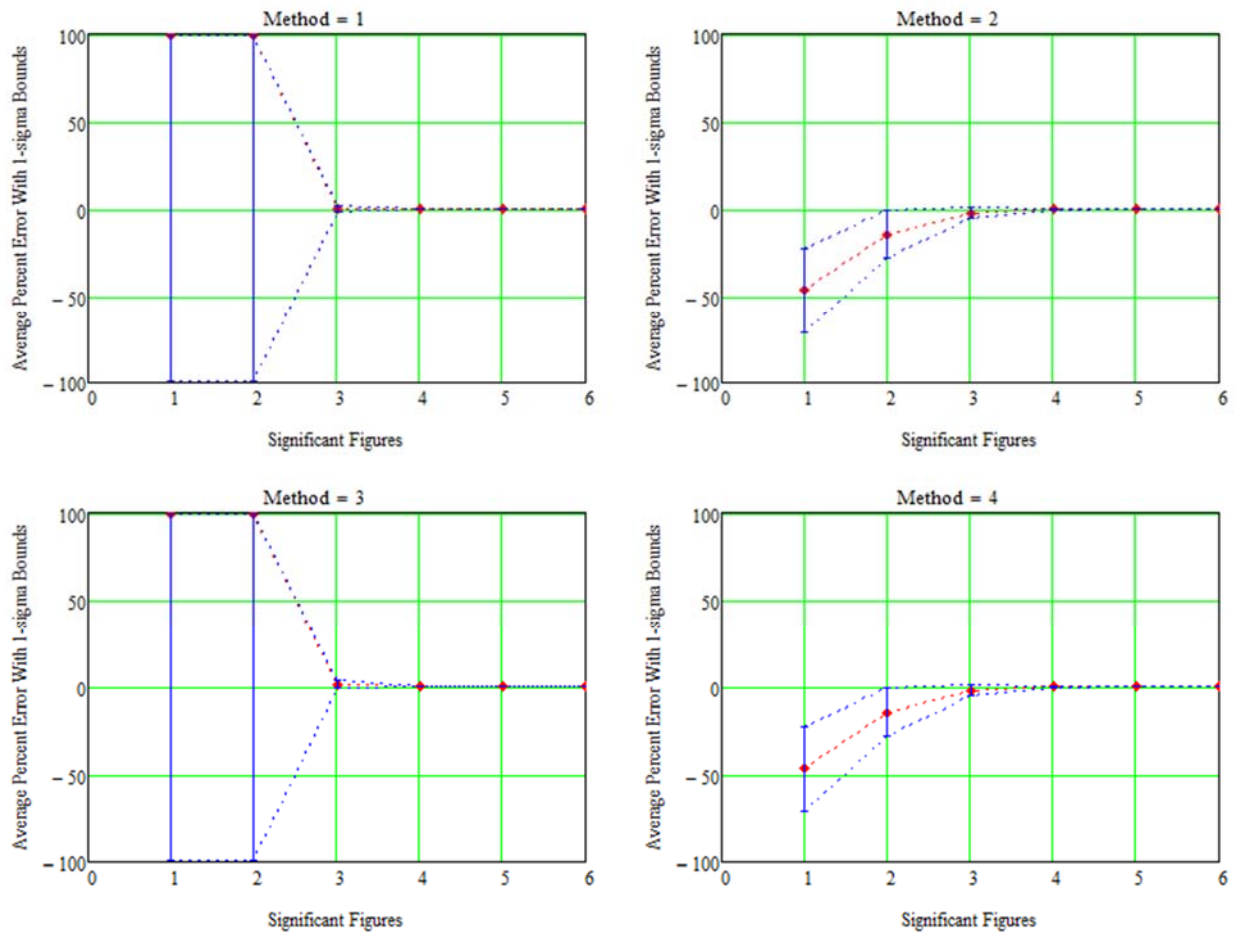


Fig. 10 Collision-probability calculation error using the four methods ( $OBJ > d$ ,  $AR=3$ ).



**Fig. 11** Collision-probability calculation error using the four methods ( $OBJ > d$ ,  $AR=5$ ).



**Fig. 12** Collision-probability calculation error using the four methods ( $OBJ > d$ ,  $AR=10$ ).

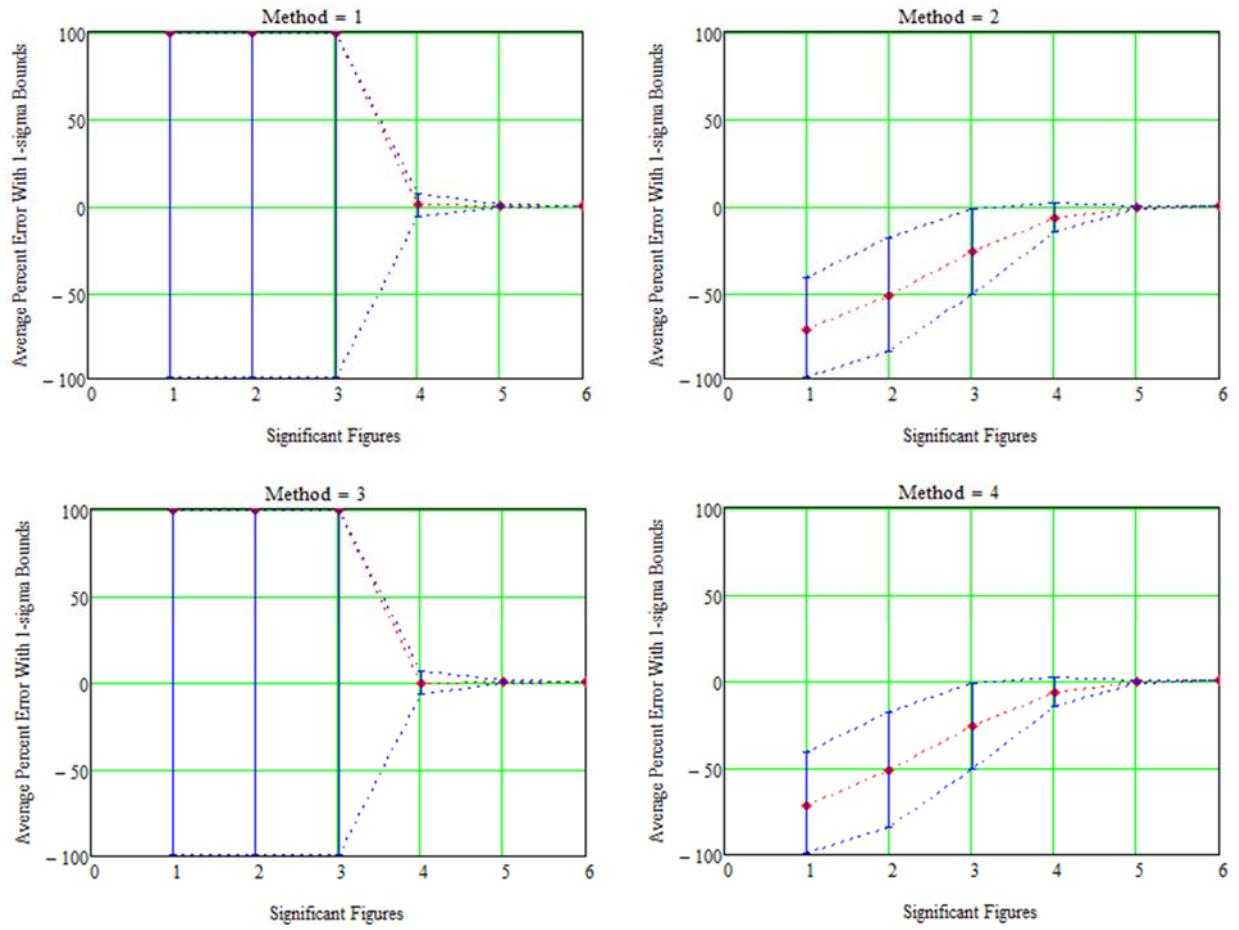


**Fig. 13** Collision-probability calculation error using the four methods ( $OBJ > d$ ,  $AR=50$ ).

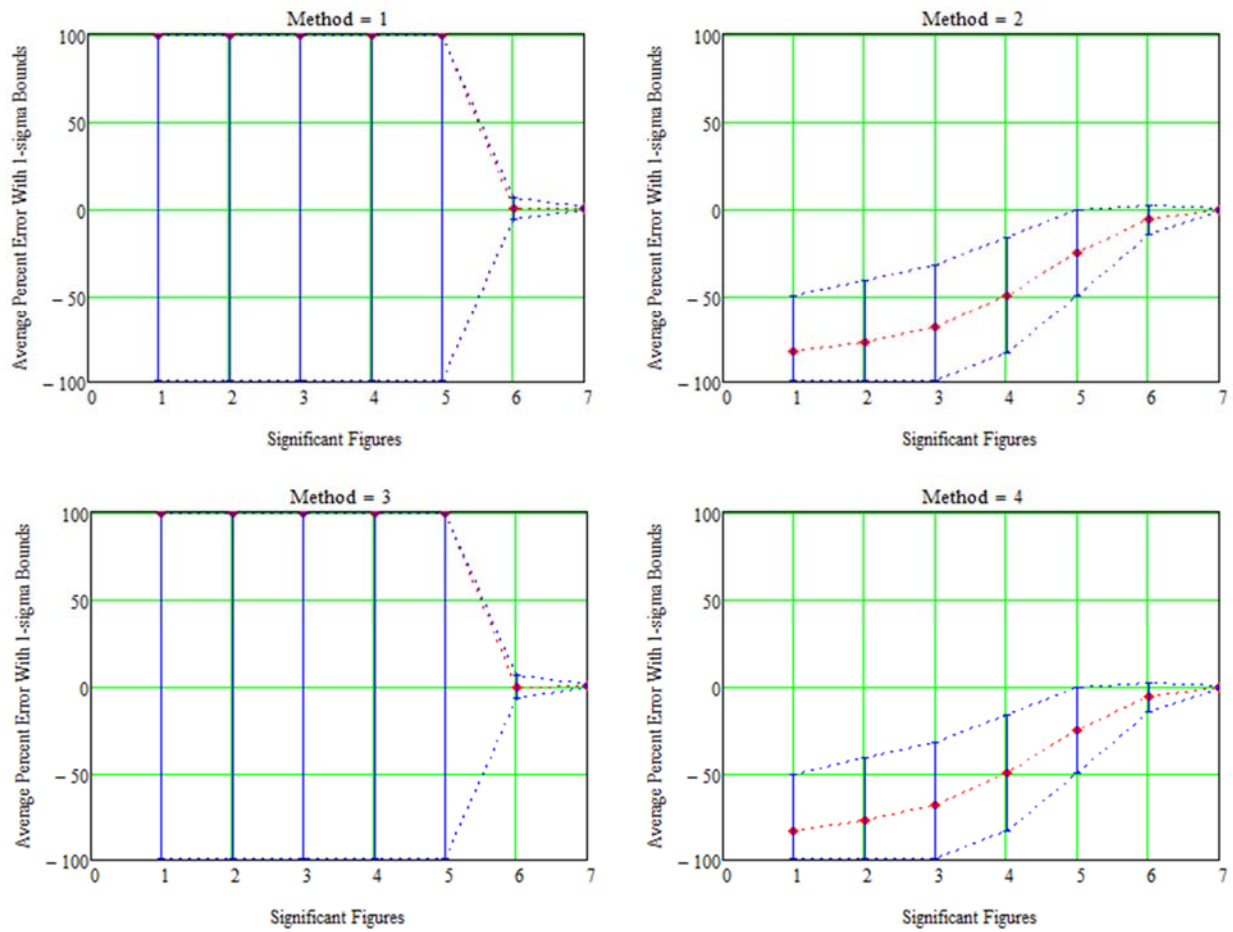


Fig. 14 Collision-probability calculation error using the four methods ( $OBJ > d$ ,  $AR=500$ ).

## Appendix C

The following figures show the effects of significant figure reduction on collision probability calculations using all four methods for collision probabilities of  $10^{-4}$  or greater:

- 1) rounding all elements,
- 2) rounding up all elements,
- 3) truncating all elements, and
- 4) the hybrid approach (rounds up diagonal elements and truncates off-diagonal elements).

After the methods were applied, the matrices that were no longer positive definite were remediated using the Eigenvalue Clipping Method. Relative percent errors of all covariance matrices (remediated and those that remained positive definite) are depicted in red. The error's one-sigma standard deviation is shown in blue. To make the plots more readable, all plots have the error data clipped at 100%.

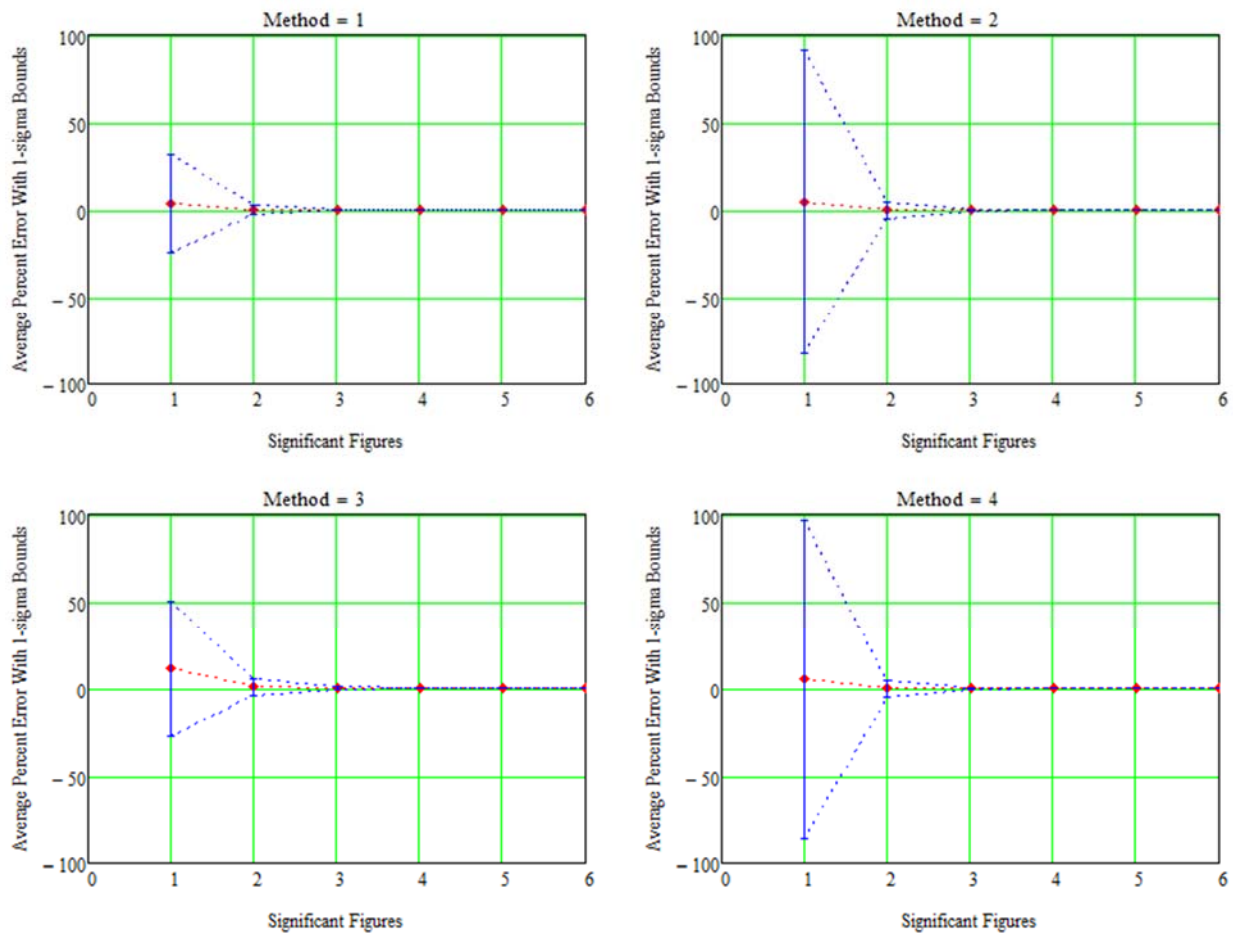
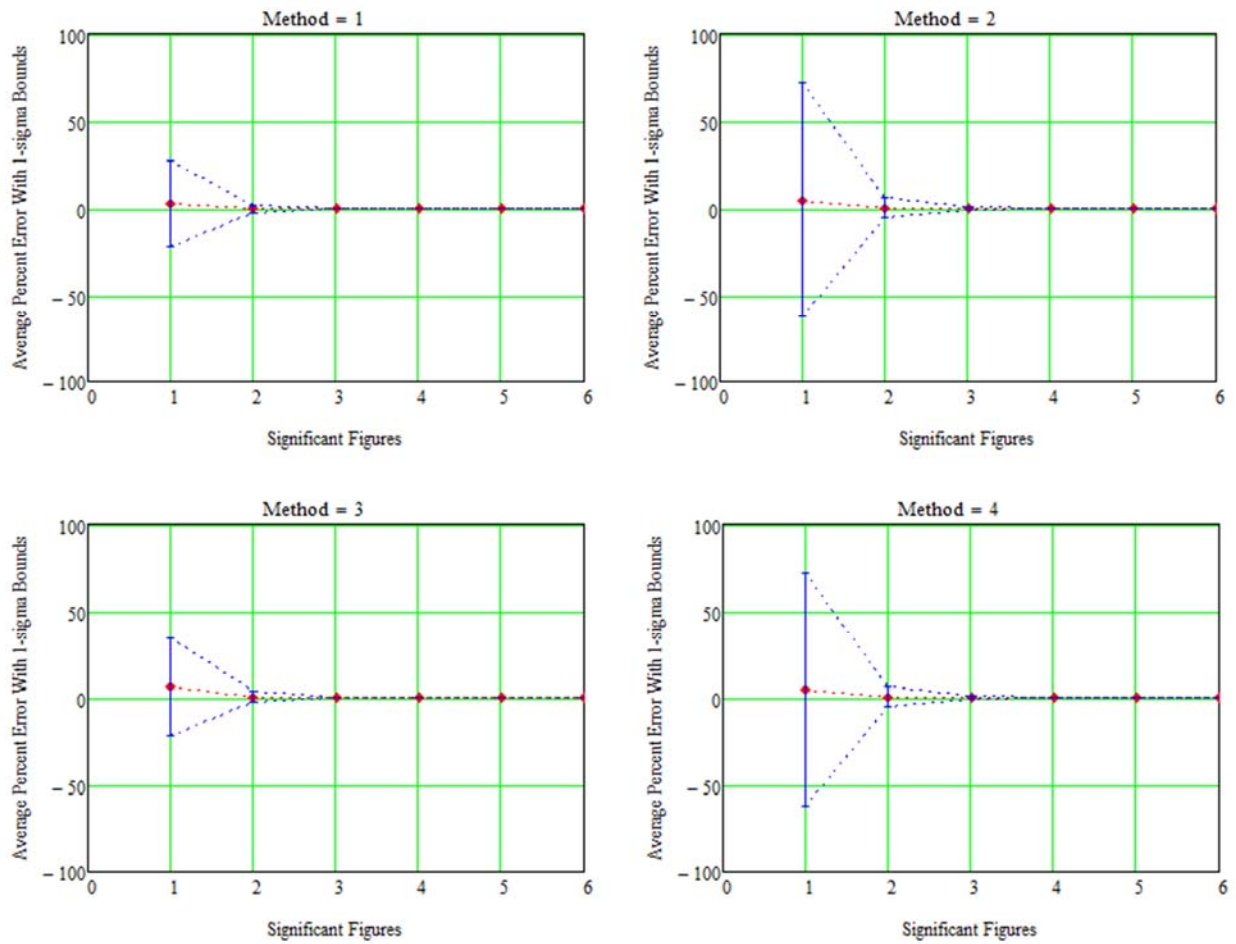


Fig. C1 Collision-probability calculation error using the four methods ( $OBJ \leq d$ ,  $AR=1$ ).



**Fig. C2** Collision-probability calculation error using the four methods ( $OBJ \leq d$ ,  $AR=2$ ).

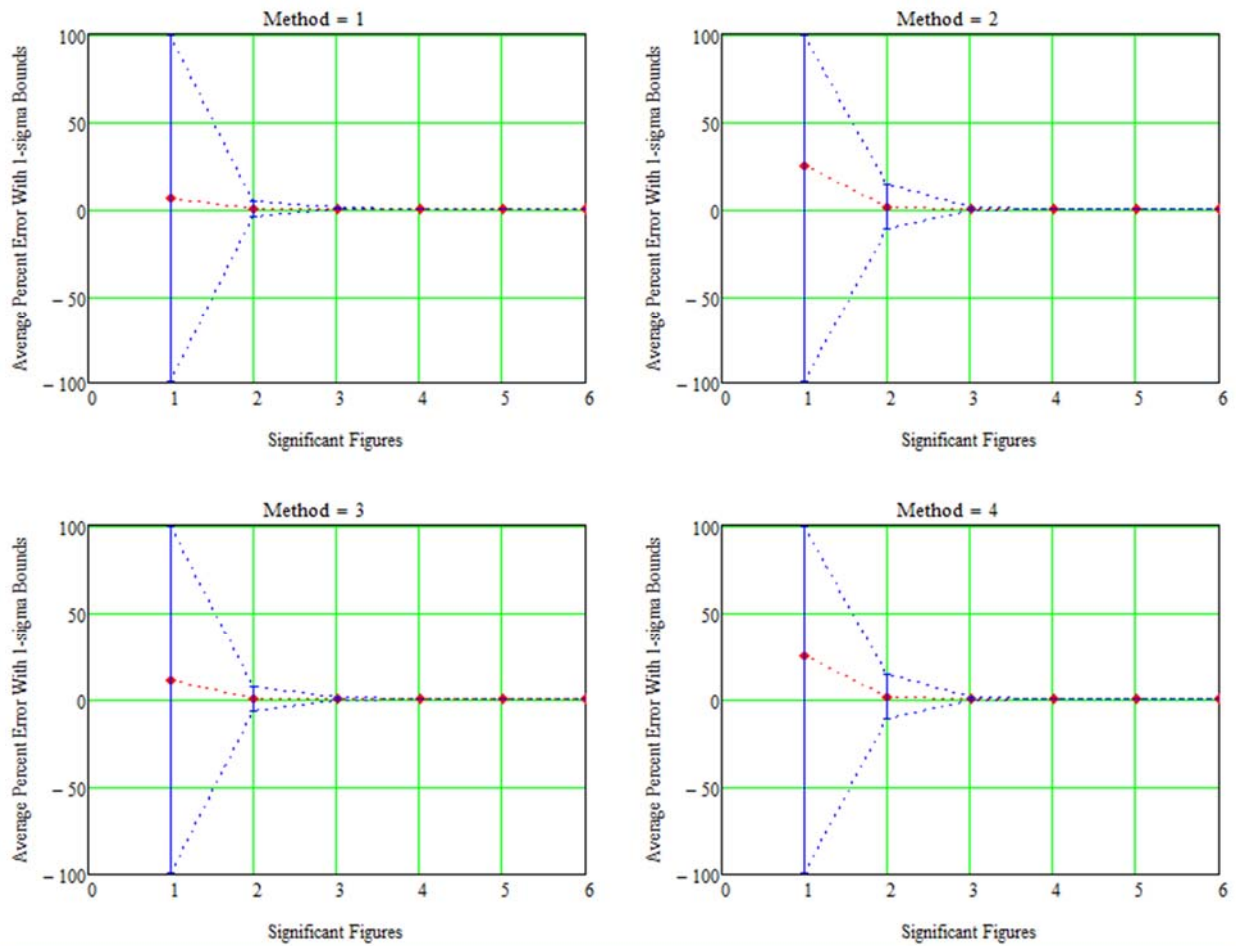


Fig. C3 Collision-probability calculation error using the four methods ( $OBJ \leq d$ ,  $AR=3$ ).

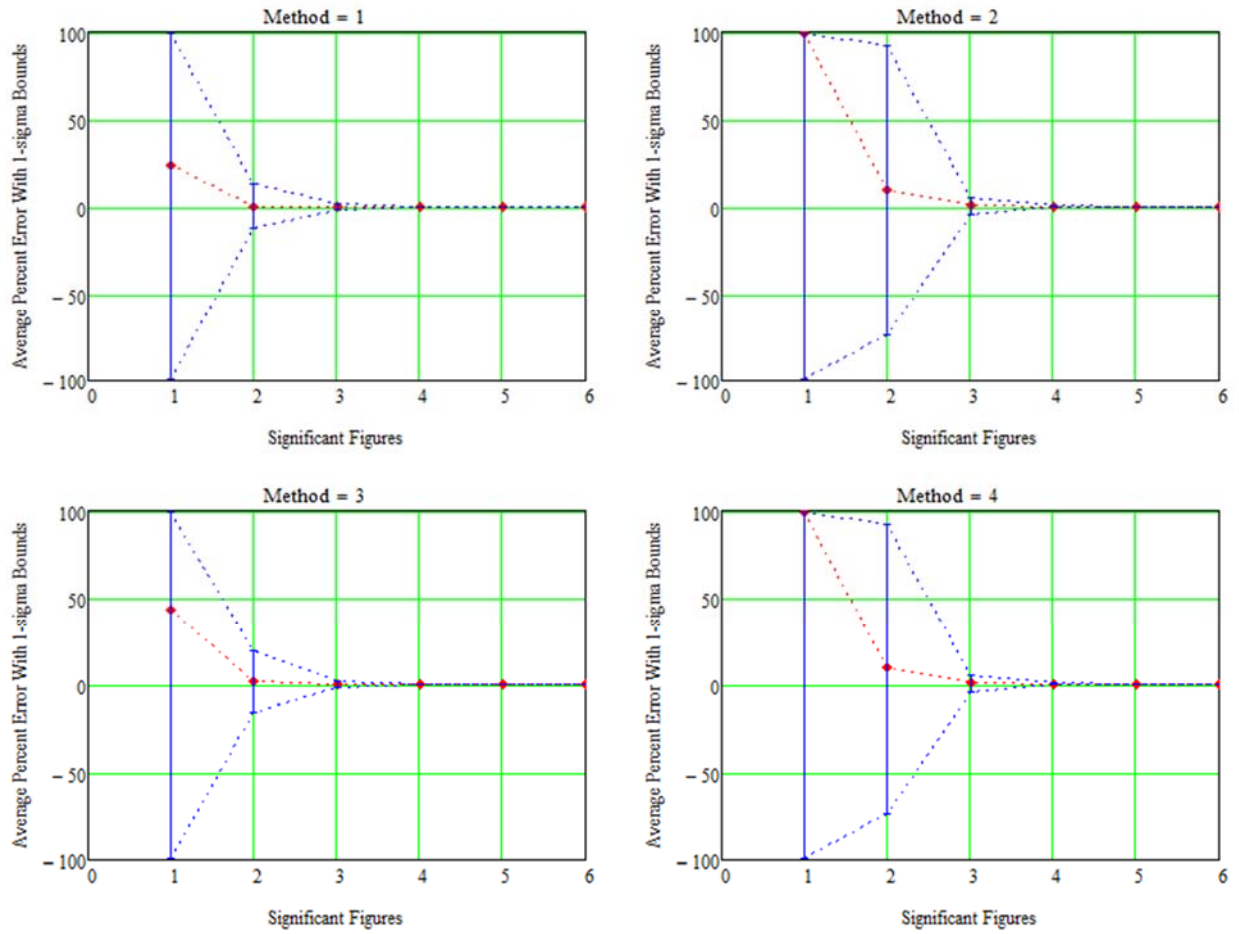


Fig. C4 Collision-probability calculation error using the four methods ( $OBJ \leq d$ ,  $AR=5$ ).

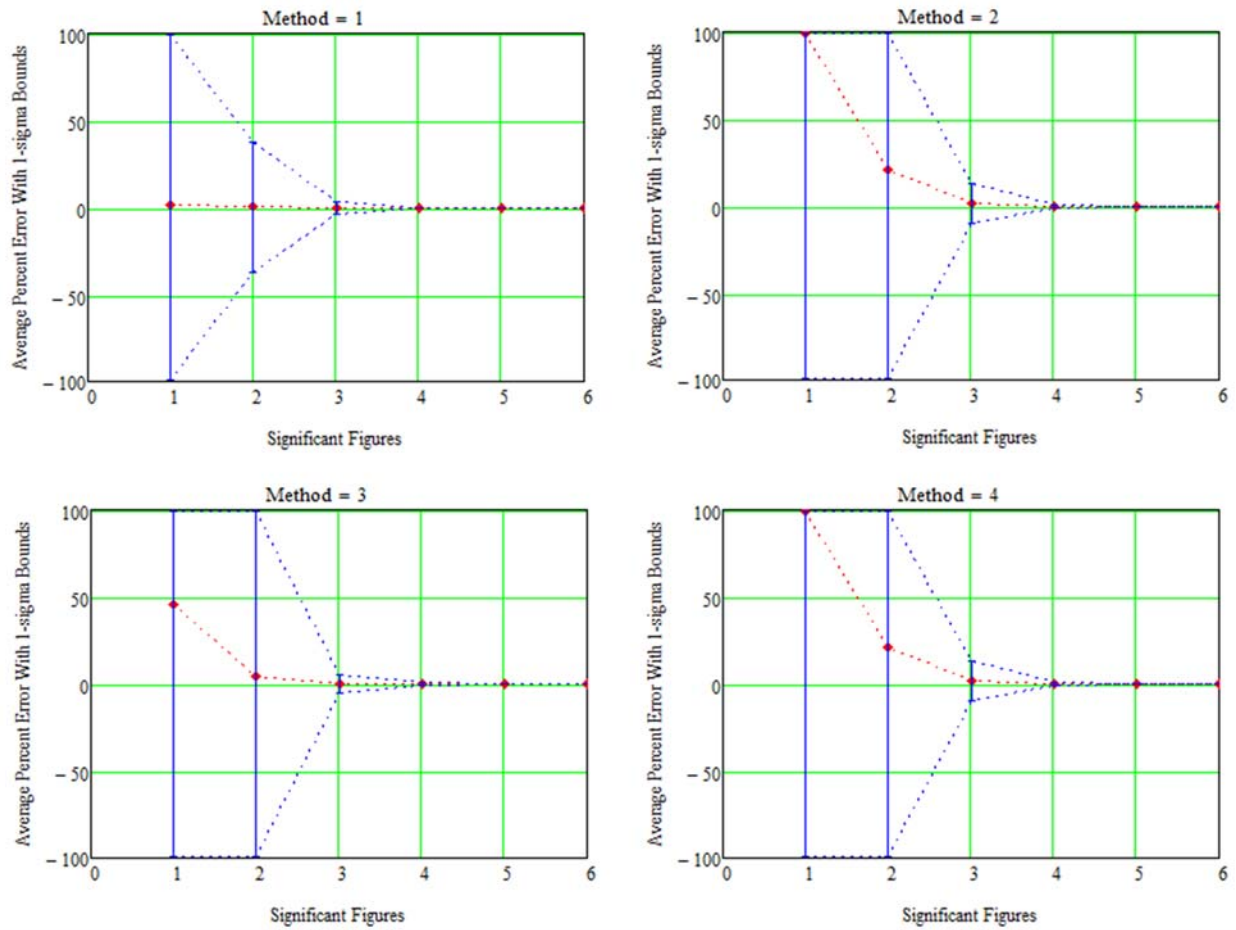


Fig. C5 Collision-probability calculation error using the four methods ( $OBJ \leq d$ ,  $AR=10$ ).

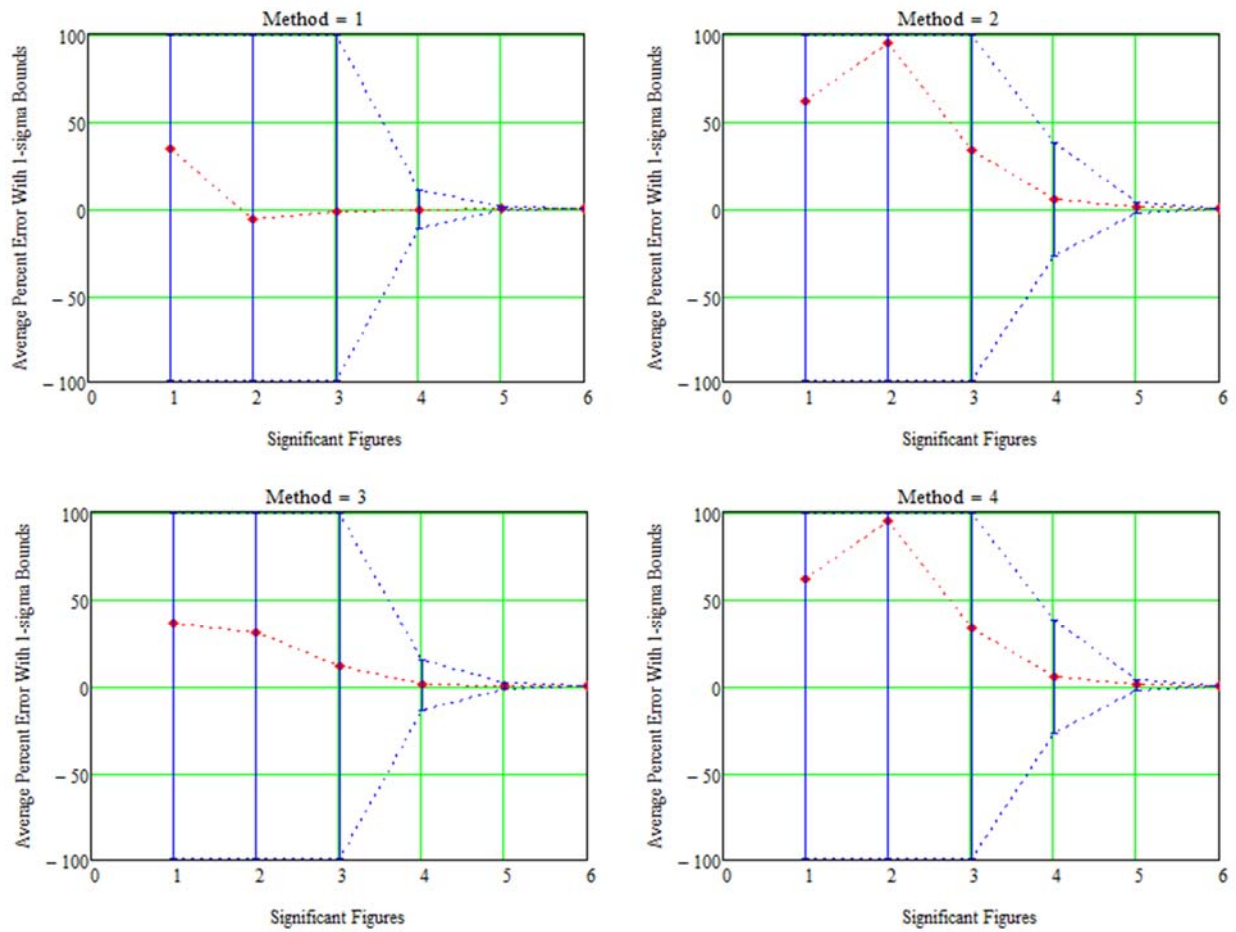
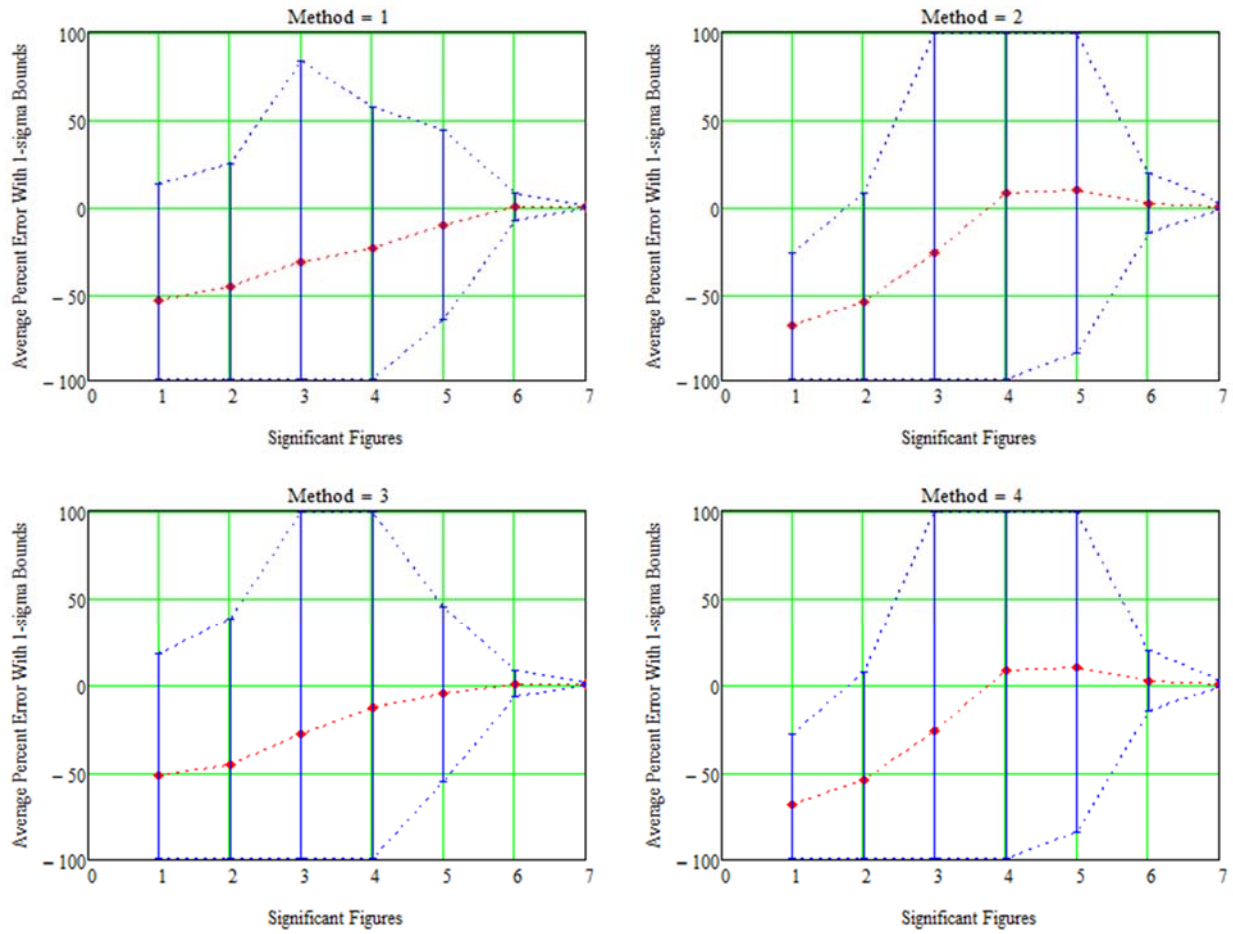
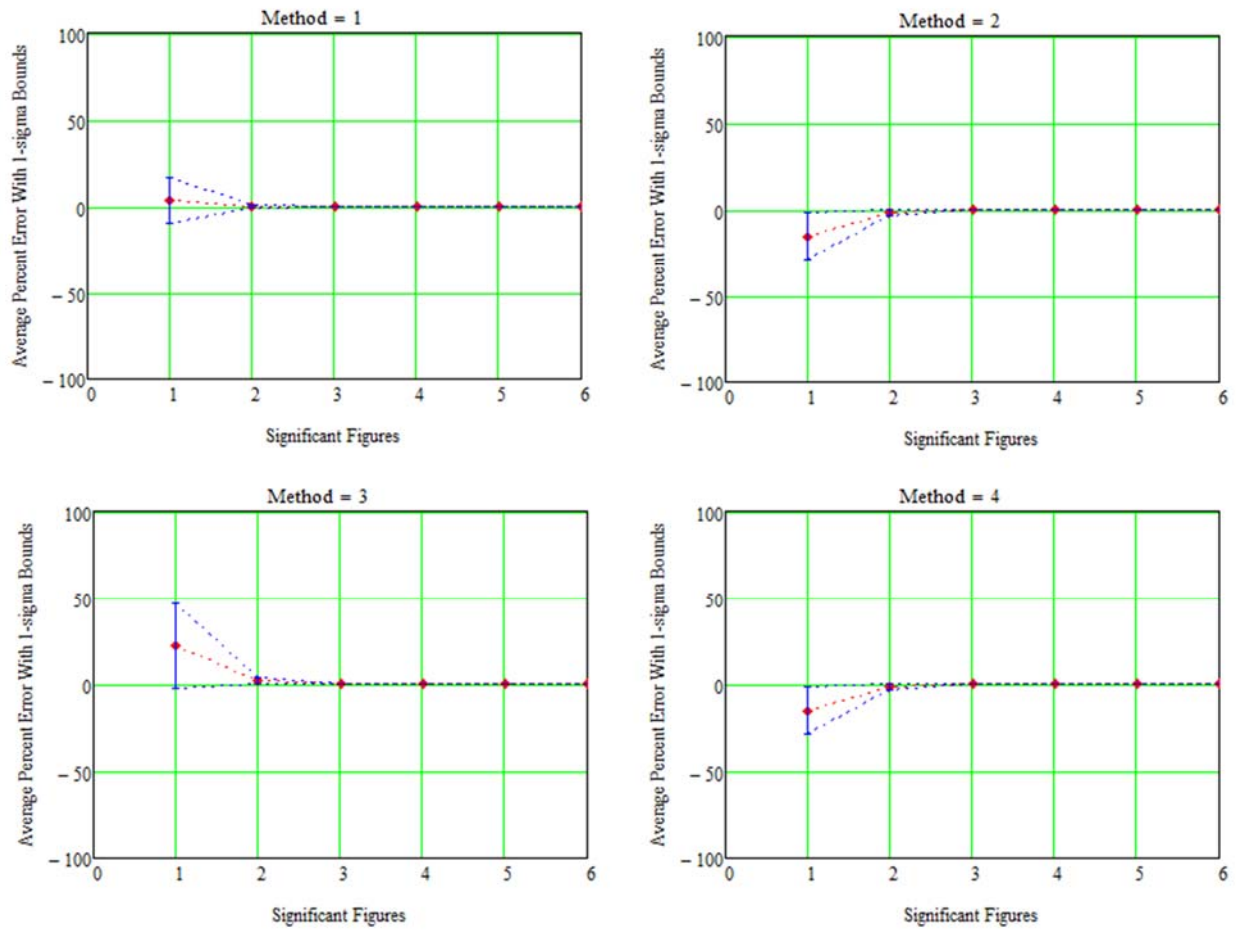


Fig. C6 Collision-probability calculation error using the four methods ( $OBJ \leq d$ ,  $AR=50$ ).



**Fig. C7** Collision-probability calculation error using the four methods ( $OBJ \leq d$ ,  $AR=500$ ).



**Fig. C8** Collision-probability calculation error using the four methods ( $OBJ > d$ ,  $AR=1$ ).

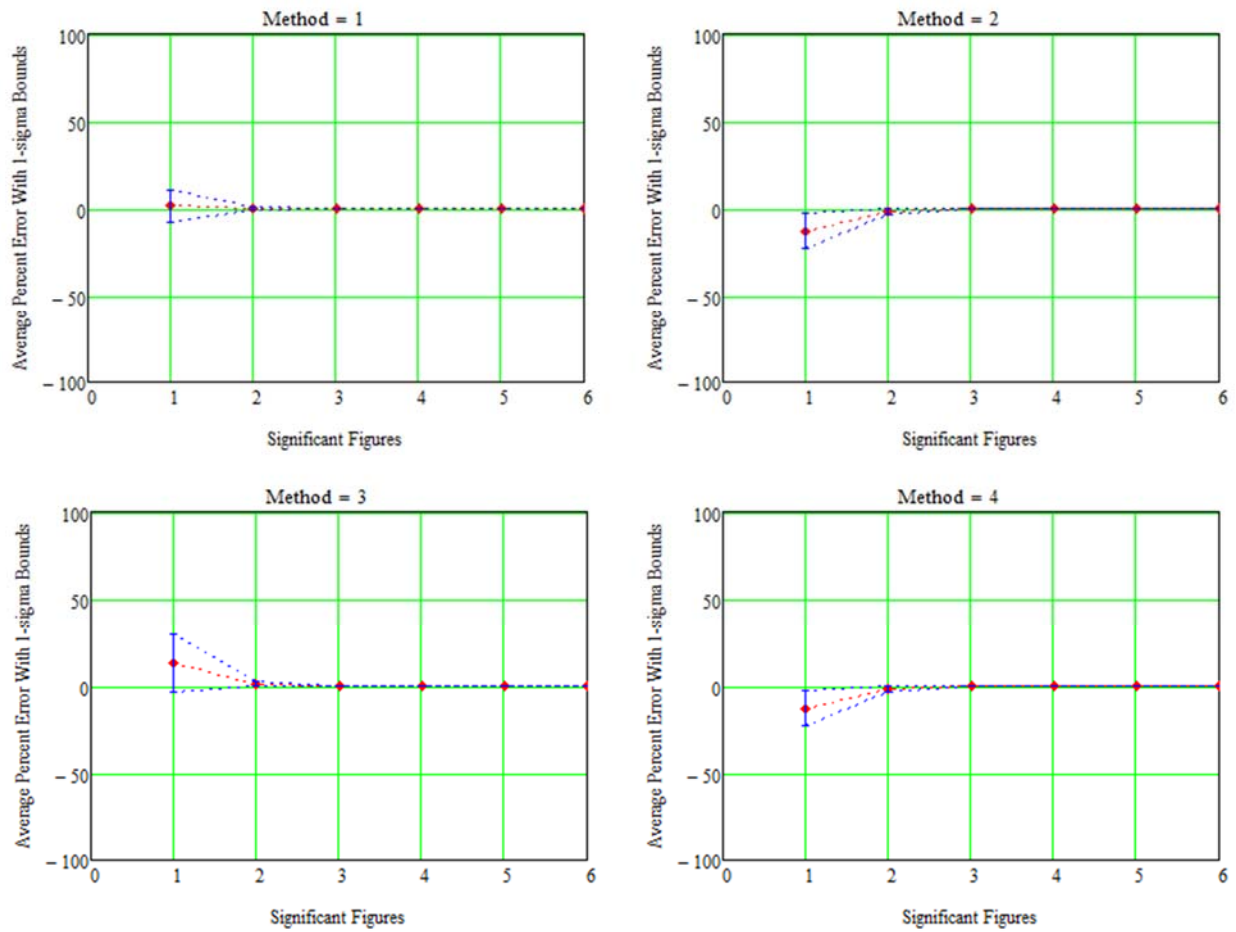
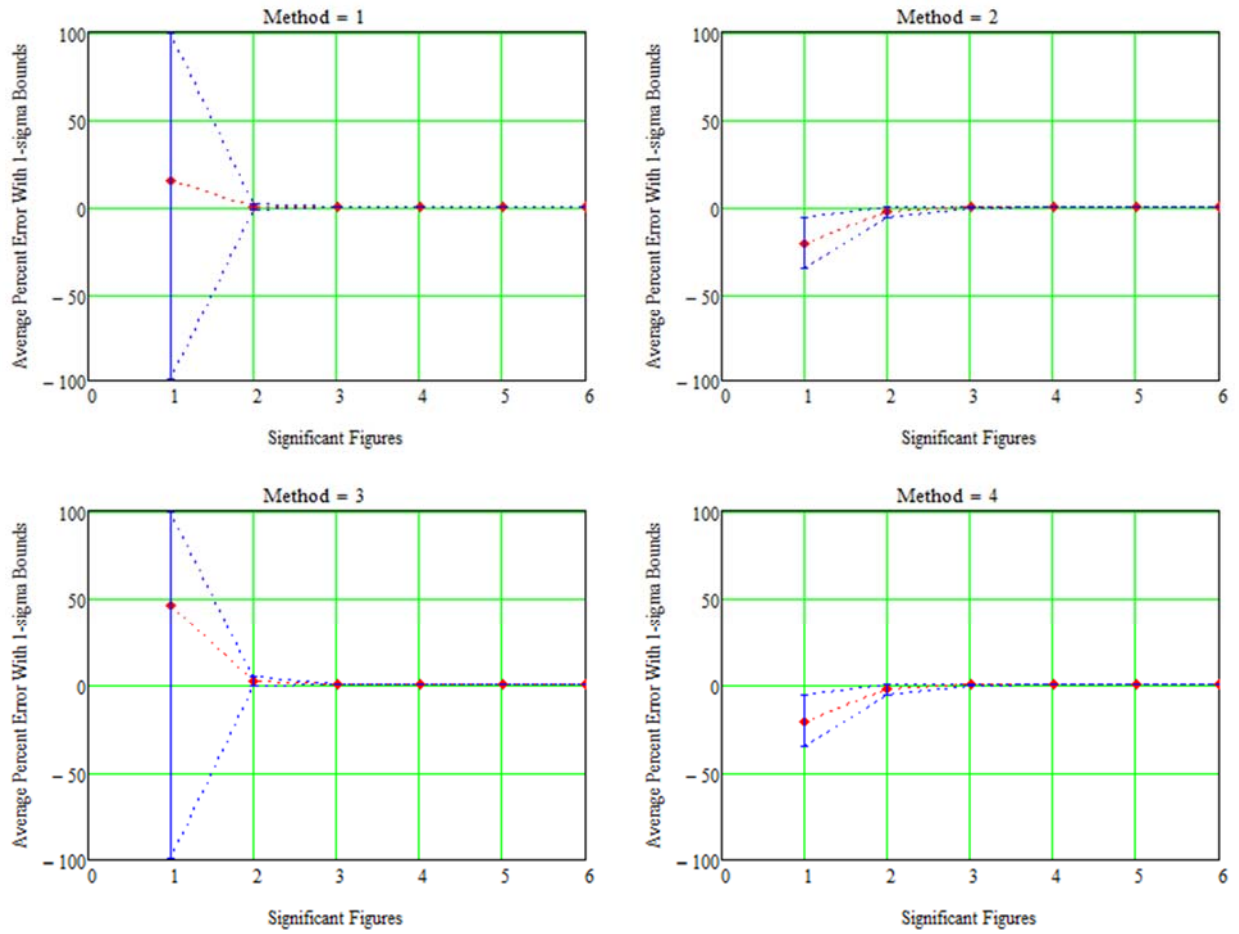


Fig. C9 Collision-probability calculation error using the four methods ( $OBJ > d$ ,  $AR=2$ ).



**Fig. C10** Collision-probability calculation error using the four methods ( $OBJ > d$ ,  $AR=3$ ).

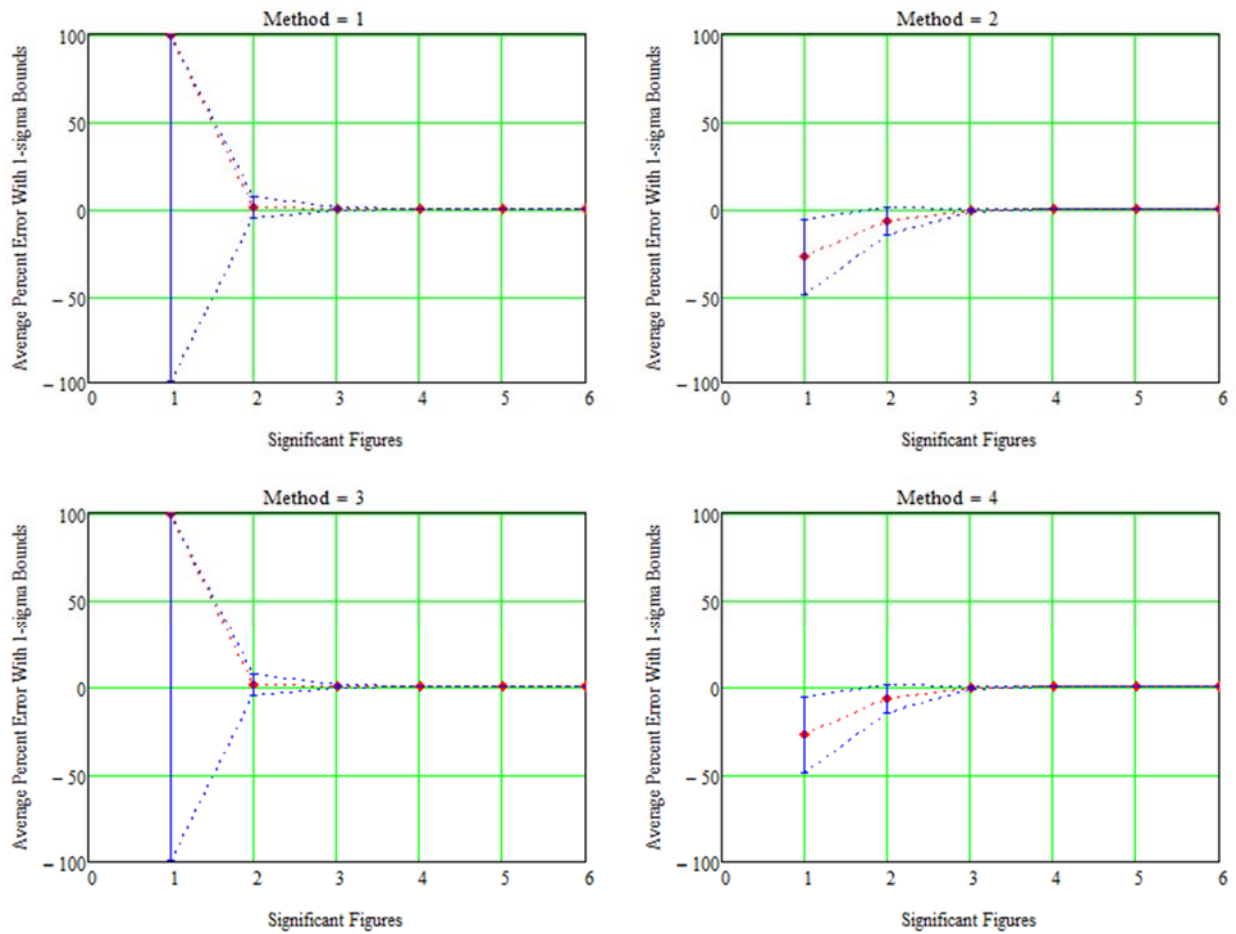


Fig. C11 Collision-probability calculation error using the four methods ( $OBJ > d$ ,  $AR=5$ ).

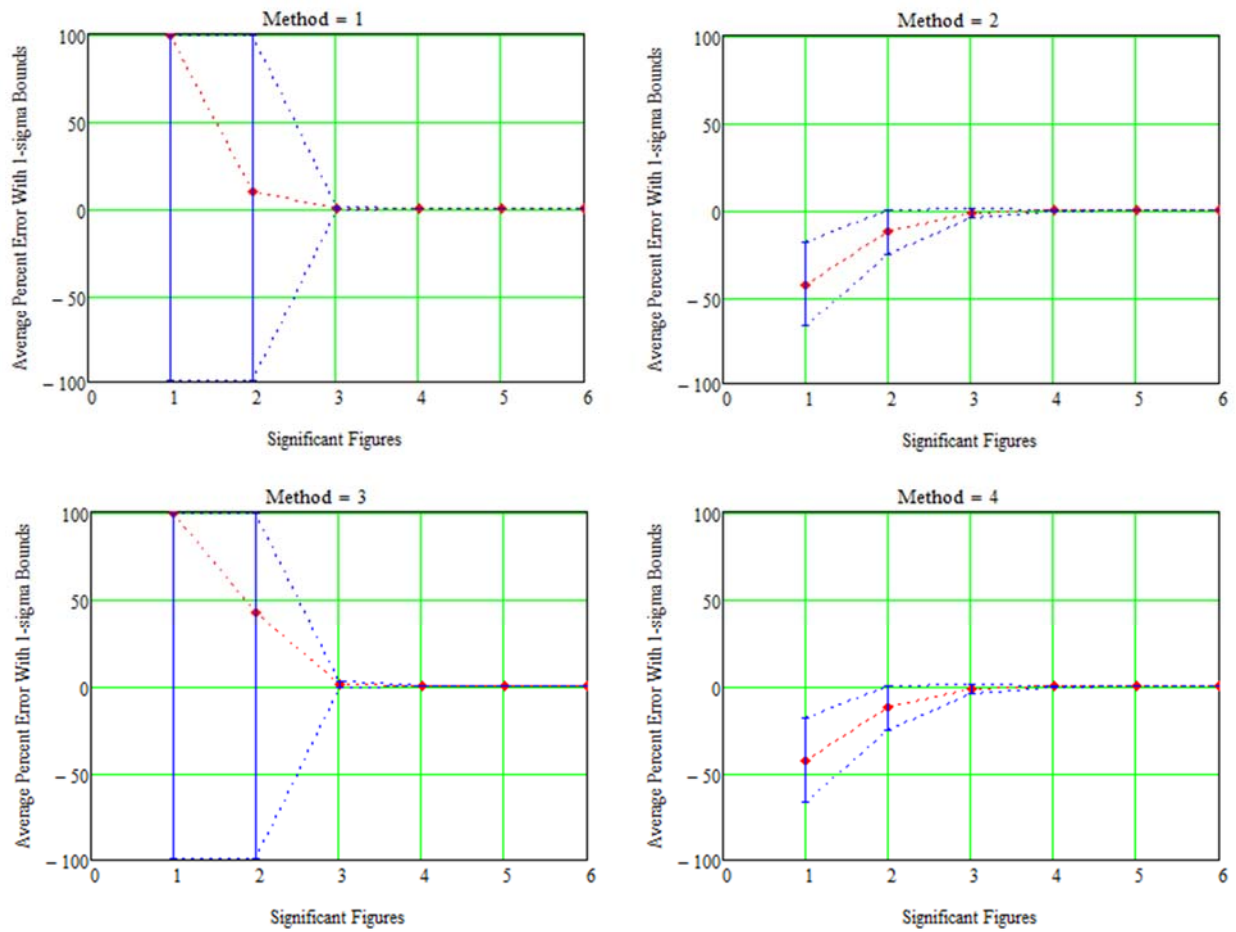


Fig. C12 Collision-probability calculation error using the four methods ( $OBJ > d$ ,  $AR=10$ ).

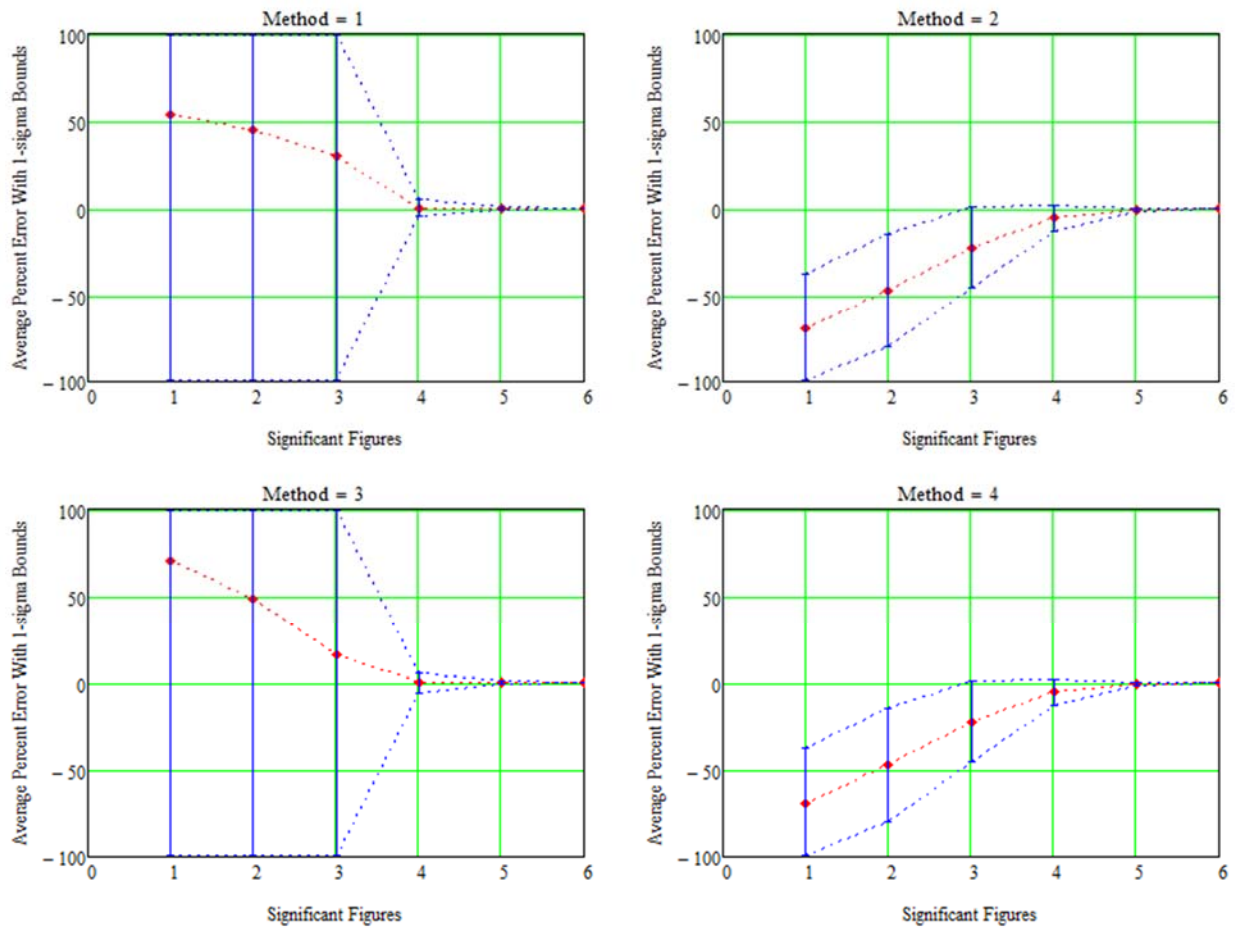


Fig. C13 Collision-probability calculation error using the four methods ( $OBJ > d$ ,  $AR=50$ ).

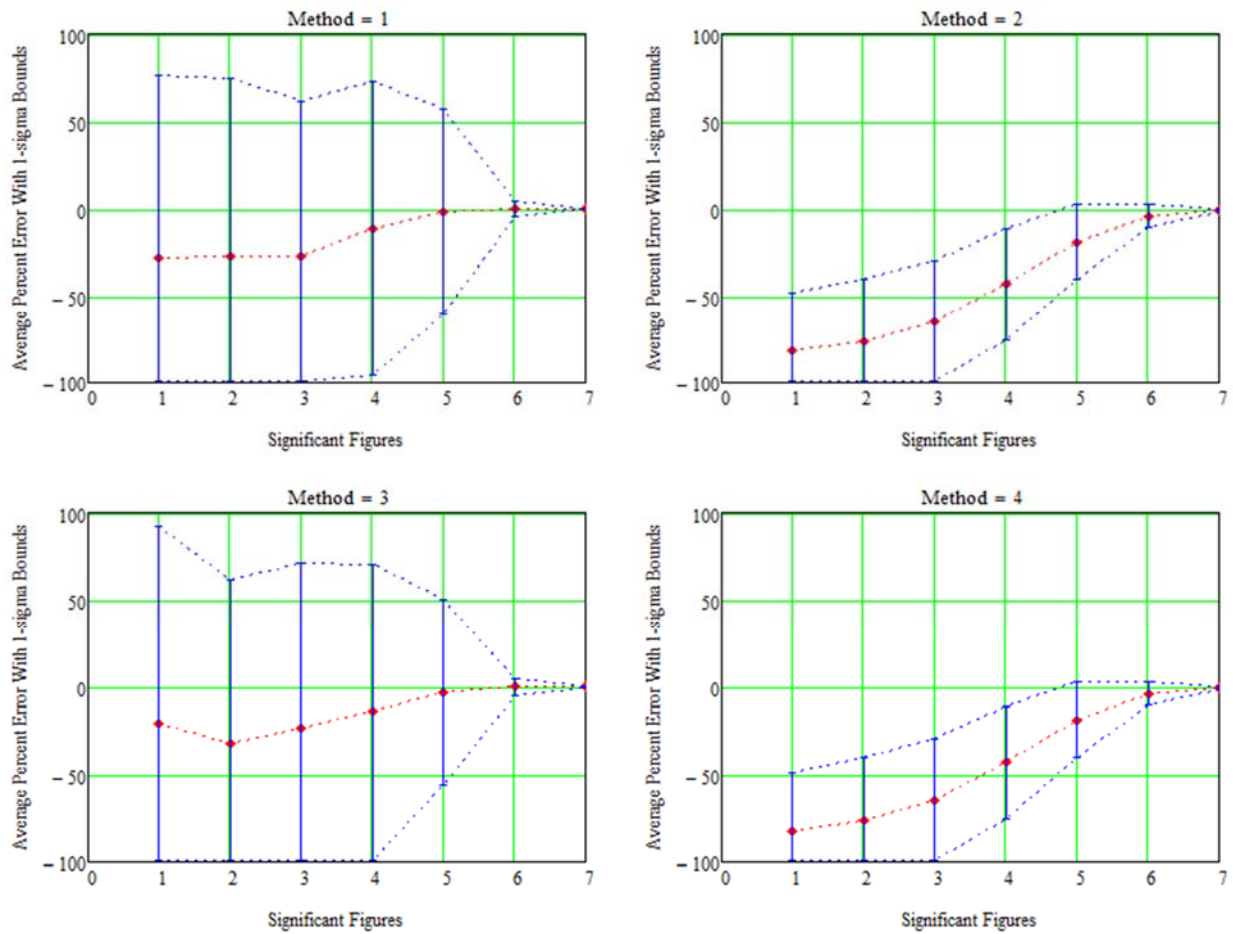


Fig. C14 Collision-probability calculation error using the four methods ( $OBJ > d$ ,  $AR=500$ ).